Energy-based cost integrated modelling and sustainability assessment of Al-GnP hybrid nanofluid assisted turning of AISI52100 steel

Khan, Aqib Mashood; Gupta, Munish Kumar; Hegab, Hussein; Jamil, Muhammad; Mia, Mozammel; He, Ning; Song, Qinghua; Liu, Zhanqiang; Pruncu, Catalin Iulian

DOI:
10.1016/j.jclepro.2020.120502

Document Version
Peer reviewed version

Citation for published version (Harvard):
Khan, AM, Gupta, MK, Hegab, H, Jamil, M, Mia, M, He, N, Song, Q, Liu, Z & Pruncu, CI 2020, 'Energy-based cost integrated modelling and sustainability assessment of Al-GnP hybrid nanofluid assisted turning of AISI52100 steel', *Journal of Cleaner Production*, vol. 257, 120502, pp. 1-17.
https://doi.org/10.1016/j.jclepro.2020.120502

Journal Pre-proof

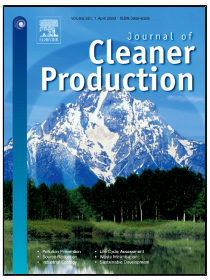

Energy-Based Cost Integrated Modelling and Sustainability Assessment of Al-GnP Hybrid Nanofluid Assisted Turning of AISI52100 Steel

Aqib Mashood Khan, Munish Kumar Gupta, Hussein Hegab, Muhammad Jamil, Mozammel Mia, Ning He, Qinghua Song, Zhanqiang Liu, Catalin Iulian Pruncu

PII:	S0959-6526(20)30549-7
DOI:	https://doi.org/10.1016/j.jclepro.2020.120502
Reference:	JCLP 120502
To appear in:	*Journal of Cleaner Production*
Received Date:	18 October 2019
Accepted Date:	08 February 2020

Please cite this article as: Aqib Mashood Khan, Munish Kumar Gupta, Hussein Hegab, Muhammad Jamil, Mozammel Mia, Ning He, Qinghua Song, Zhanqiang Liu, Catalin Iulian Pruncu, Energy-Based Cost Integrated Modelling and Sustainability Assessment of Al-GnP Hybrid Nanofluid Assisted Turning of AISI52100 Steel, *Journal of Cleaner Production* (2020), https://doi.org/10.1016/j.jclepro.2020.120502

Graphical Abstract

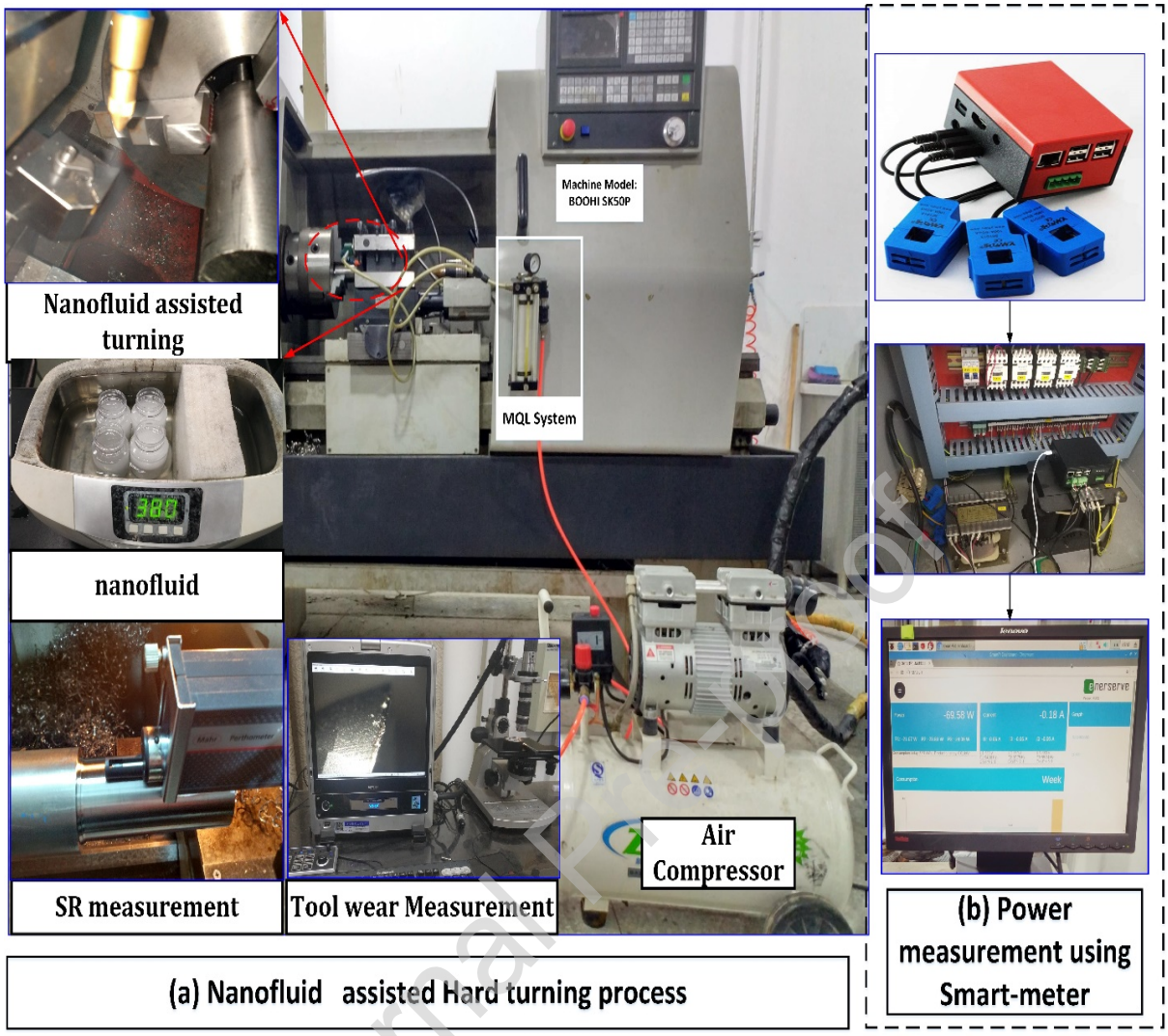

Energy-Based Cost Integrated Modelling and Sustainability Assessment of Al-GnP Hybrid Nanofluid Assisted Turning of AISI52100 Steel

Aqib Mashood Khan[1,2], Munish Kumar Gupta[3], Hussein Hegab[4], Muhammad Jamil[1,2*], Mozammel Mia[5], Ning He[1,2], Qinghua Song[3,6*], Zhanqiang Liu[3,6], Catalin Iulian Pruncu[5,7]

[1]College of Mechanical and Electrical Engineering, Nanjing University of Aeronautics and Astronautics NUAA, Nanjing 21000, China. dr.aqib@nuaa.edu.cn; engr.jamil@nuaa.edu.cn

[2]National Engineering Research Center for Processing of Difficult-to-Machine Materials, College of Electrical and Mechanical Engineering, Nanjing University of Aeronautics and Astronautics NUAA, Nanjing 21000, China.

[3]Key Laboratory of High Efficiency and Clean Mechanical Manufacture, Ministry of Education, School of Mechanical Engineering, Shandong University, Jinan, P.R. China. munishguptanit@gmail.com; https://orcid.org/0000-0002-0777-1559

[4]Mechanical Design and Production Engineering Department, Cairo University, Giza 12163, Egypt; hussien.hegab@uoit.ca

[5]Mechanical Engineering, Imperial College London, Exhibition Road, South Kensington, SW7 2AZ, London, United Kingdom; m.mia19@imperial.ac.uk, https://orcid.org/0000-0002-8351-1871

[6]National Demonstration Center for Experimental Mechanical Engineering Education, Shandong University, Jinan, P.R. China, ssinghua@sdu.edu.cn, melius@sdu.edu.cn.

[7]Mechanical Engineering, School of Engineering, University of Birmingham, Birmingham B15 2TT, UK, c.pruncu@imperial.ac.uk

***Corresponding author: (Q. Song) ssinghua@sdu.edu.cn, (M. Jamil) engr.jamil@nuaa.edu.cn**

Abstract:

The need of a cost-effective production system is indispensable, especially in the current competitive manufacturing market. To the same extent, special attention should be focused on the sustainable and clean machining processes. Several studies have focused on the machining of hard-to-cut materials using sustainable and clean cutting technologies. However, there is a need to establish a detailed and reliable cost-energy model for sustainable machining processes. In this research, empirical models have been developed for cost and energy consumption to define the system boundaries under different cooling conditions. Mono and hybrid nanofluids have been synthesized and their performance is evaluated by analyzing viscosity, thermal conductivity, and coefficient of friction. Moreover, a holistic sustainability assessment has been performed for the measured results. The surface roughness, power and energy consumption, tool life and cost per part are determined and the results are compared with those obtained in classical MQL process. It should be noted that the study findings offer guidelines which can be easily implemented in any metal processing industry to enhance the process's performance measures. Furthermore, this work is the first of its kind that proposes hybrid Energy-Cost models and their experimental validations.

Keywords:

Sustainability; Energy; Machining cost; Tool wear; Machining; Hybrid nanofluid.

List of Abbreviations and Symbols

Abbr.	Meaning	Abbr.	Meaning
MQL	Minimum quantity lubrication	NFMQL	Mono nanofluid assisted MQL
HNFMQL	Hybrid nanofluid assisted MQL	EIA	Energy information administration
EPA	Environmental Protection Agency	Al-GnP	Alumina- Graphene nanoparticles
DI-water	Deionized Water	BUA	Bottom-up Approach
SCE	Specific Cutting Energy	SEC	Specific Energy Consumption
CoF	Coefficient of Friction	MRV	Material removal Volume
EC	Energy consumption	CES	Carbon emission Signature
C_P	Cost per part	OPI	Overall Performance Index
n_p	Nanoparticles concentration	v_c	Cutting speed
f	Feed rate	a_p	Depth of cut
Db	Brownian diffusion coefficient	T	Temperature
μ	Viscosity	dP	Diameter of nanoparticles
CoF	Coefficient of friction	t_i	Idle time
t_{sb}	Standby time	t_c	Cutting time
t_a	Air cutting time	t_{lub}	Lubrication time
$t_{tc/p}$	Tool change time per part	t_h	Material Handling time
t_{su}	Setup time	t_{suw}	Workpiece setup time
t_{sut}	Tool setup time	T_L	Tool life
N	No. of part per cutting tool	l_c	Cutting length
l_a	Air cutting length	P_{sb}	Standby power
P_a	Air cutting power	P_c	Cutting power
P_{tc}	Tool change power	P_{lub}	Lubrication power
P_t	Total power	P_m	Machining Power
C_P	Cost per part	C_e	Energy cost
C_m	Machining cost	C_{CT}	Cutting tool cost
C_f	Total cost of fluid consumed	C_w	Workpiece cost
C_{np}	Cost of nanoparticles	h_e	Machining cost rate
X_e	Unit electricity cost	X_{CT}	Cutting tool cost
X_f	Cost per unit consumption of Fluid		

1. Introduction

Recently, the concept of energy-saving, pollution control, health issues, and environmental concerns have become more prevalent globally. The pressure to reduce these concerns is promoted by the governments (Campitelli et al., 2019). According to an international survey, 542 quadrillions Btu global energy was only consumed in 2010, and its estimated value will reach up to 630 quadrillions Btu in 2020 (Bagaber and Yusoff, 2019). It is revealed in another report related to the carbon emissions for 2015 that a total of 4997 million metric tons of the emissions have been released in the USA, while 9084.6 million metric tons have been released in China (U.S., 2009). According to the statistics of the US Energy Information Administration (EIA), the metal products fabrication industry consumes 47 billion kWh, which represents about 45% of the total power consumed in the entire industry (EIA, 2013). Therefore, it is important to develop new technologies that can achieve better energy efficiency and reduce energy consumption within manufacturing processes.

When talking about machining operations, the turning, milling, and drilling processes have frequently been employed to achieve high-quality products. Among these, the turning process has some distinct features that enable us to achieve precise and complex cylindrical shapes. Lately, a significant improvement in tool materials, parameters control, and cooling/lubrication (lubricooling) factors have led to an efficient machining process (Gupta et al., 2016a; Mia et al., 2019)In turning operation, the high level of temperature generated at the workpiece-tool interface is linked to high hardness, and inferior thermal conductivity of materials. In order to deal with the heat generation and process efficiency issues, the conventional cooling (flood approach) has frequently been applied with excessive usage of mineral-based lubricants. It is considered as an effective solution to the high generated heat, however it causes serious health concerns, jeopardizing green manufacturing and sustainability (Said et al., 2019).

Sustainable manufacturing is the latest concept in the modern industrial sector. It permits shifting the machining sector from a "conventional based environment" to a "sustainable based environment", using strict rules that allow identification of various skin allergic diseases as per Environmental Protection Agency (EPA) regulation (Liang et al., 2019). The proper implementation of the sustainability aspects will be reflected in the entire economy in the manufacturing industry. The enormous quantity of chemical liquids is used for achieving lubrication and cooling which enables the machining process to sustain aggressive cutting conditions. It is roughly estimated that 640 million gallons of cutting fluids have been annually used for manufacturing purposes (Kaliszer, 2003). To mitigate the common workshop floor allergic effects of nondegradable lubricants, a milestone was achieved through the Minimum Quantity Lubrication (MQL) system. MQL system helps to reduce the quantity of lubricant without compromising the productivity of the process. Therefore, the MQL approach can be accepted as a viable option to resolve the problems associated with the nondegradable lubricants (Cabanettes et al., 2017).

MQL is based on using the optimized lubricant quantity to lubricate the cutting zone (Sarikaya and Güllü, 2015, 2014; Sarıkaya et al., 2016). It reduces the overall machining cost (15-17%) by reducing the cost of lubricant (Filipovic and Stephenson, 2006). Biocut and Blasocut mineral oils are used to lubricate, and evacuate heat from the cutting zone (Maruda et al., 2016). Lugscheider et al. (1999) used micro-lubrication when reaming cast iron. Results showed a considerable reduction of cutting tool wear and surface roughness in comparison with the dry cutting environment. Researchers conducted drilling tests under the MQL approach with a flow rate of 10-15 mL/h. The mist was delivered around the chip-tool contact zone to achieve the superior surface finish and longer tool lifespan (Klocke and Eisenblaetter, 1997). Sani et al. (2019) investigated the machining quality when using vegetable oil combined with ammonium-based ionic liquids through the MQL system. The findings revealed that the ionic liquids are suitable for improving the machining

characteristics, and they are considered as a cleaner alternative for machining AISI 1045 steel.

Lawal et al. (2013) compared some sustainable lubrication techniques available in machining. The review suggested a significant potential to use MQL with vegetable oil as it provides a biologically inert and non-toxic alternative as cutting fluids, and features much better compared to the mineral-based one. Khan et al. (2009) used micro-lubrication with vegetable oil during machining AISI-9310 steel. The achieved results demonstrated a better surface finish, smoother and brighter chip when compared with the typical dry and wet cutting environment. Moreover, lower flank wear was detected using vegetable oil-based micro-lubrication. Sharma et al. (2015) reported that the base lubricant has a key role in achieving better tribological and thermal properties by mixing nanoparticles.

The promising performance of nanofluids assisted MQL was associated with lower cutting forces, surface roughness, tool wear and temperature when compared to dry machining. It was mentioned that increasing nanoparticle concentration leads to high conductivity, viscosity, density, as well as generating superior heat extraction compared to the base cutting fluid. The mechanism of heat extraction, and friction reduction is mainly due to the ball-bearing effect, tribo-film polishing, sliding and rolling effects (Lee et al., 2009). Similarly, Gupta et al., (2016b) performed different experiments on titanium (grade-2) alloy using Graphite, Aluminum Oxide and Molybdenum Disulfide nanofluids. The results revealed that the graphite-based nanofluids are suitable for improving the machining characteristics. Similarly, Su et al. (2016) also evaluated the performance of graphite-based cutting fluids in turning of medium steel made of AISI 1045. The findings revealed the graphite formed with cutting fluids base is a good alternative to improve the machining performance.

2. Research objectives

From the literature, very limited work was made to demonstrate the benefits of the hybrid nanofluid MQL (HNFMQL) approach related to the sustainability

assessment in the machining process. This research is unique because it presents a holistic understanding of energy consumption associated with the carbon footprints and economics of the machining process. To sum up, the main objectives are;

- Mono and hybrid nanofluids are synthesized and their performance was analyzed.
- The nanofluid samples were evaluated for thermal conductivity performances and viscosity characteristics.
- A new model for electrical energy consumption and production cost estimation has been developed and applied in an industrial case study.
- Evaluation of three lubrication approaches for sustainable metrics was performed and compared.
- A sustainability assessment of different MQL assisted lubrication systems was performed based on the 3E (Energy, Environment, and Economy) approach.

3. Materials and Methods

3.1 Work material, machine tool and cutting tool

The turning experiments were performed on hardened-steel workpiece material with the hardness of 48 HRC and dimensions of 40 mm diameter and 100 mm length. A CNC lathe machine (BOOHI SK50P) was used to perform all turning experiments. The uncoated carbide inserts (YG8) were used as cutting tool materials, manufactured by Zhuzhou Cemented Carbide Cutting Tools Co., Ltd China. The rake angle of the tools is 0° and the relief angle of the tools is 11°. Fig. 1 shows the experimental setup and response measurements.

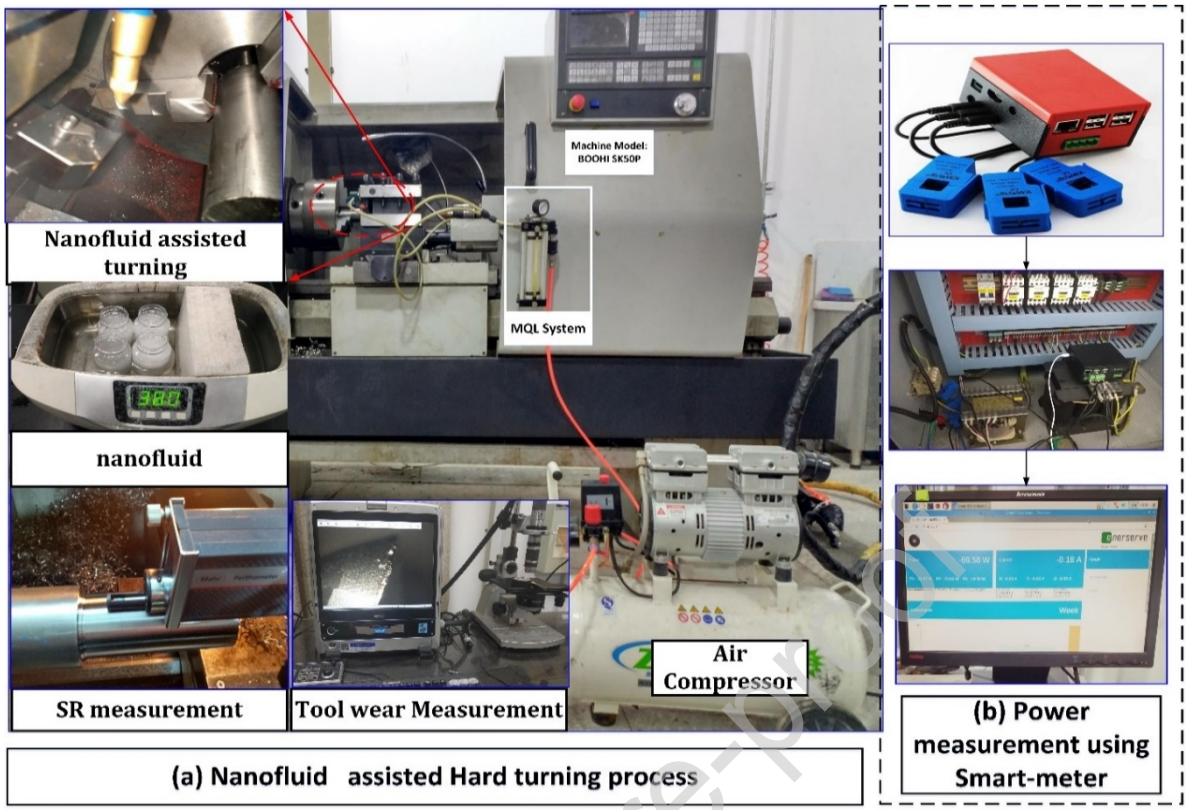

Fig. 1. Machining setup and response measurement.

3.2 Experimental design and cutting conditions

Three different types of cutting fluids (base fluid, base fluid with Al_2O_3 nanoparticle, and hybrid nanofluid with Al-GnP nanoparticle) were used with a fixed level of fluid flow rate of 300 mL/h, and compressed air at 6 bars. The length-of-cut of 100 mm, cutting depth of 0.5 mm and feed 0.1 *mm/rev* were kept constants. The variable Material Removal Rate (MRR) and Material Removal Volume (MRV) were calculated according to Eqns. (1) and (2).

$$\text{MRR} = v_c \times v_c \times a_p \quad (1)$$

$$\text{MRV} = v_c \times f \times a_p \times t_c \quad (2)$$

where, v_c represents the cutting velocity, f represents the feed rate, and a_p represents the cutting depth, and t_c represents the cutting time. Table 1 presents the cutting

parameters along with their levels and ranges. These values were set with respect to the literature review and some preliminary trials (Zhang et al., 2018).

Table 1. Cutting Parameters details along with their levels

Parameters	Symbol	Units	Level 1	Level 2	Level 3
Nanofluids type	-	type	MQL	Al_2O_3 based	Al-GnP based
Nanoparticles concentration	n_p	vol. %	0.20	0.75	1.20
Cutting speed	v_c	m/min	30	60	90
Feed rate	f	mm/rev		0.10	
Cutting depth	a_p	mm		0.5	

3.3 Measurement procedure

In the current study, the Mehr Profilometer was used to detect the average values of surface roughness (R_a). The surface roughness was measured at three different locations to determine the mean value. The flank wear (V_B) and crater wear were measured using the KEYENCE VHX-500 microscope. The nanofluids' thermal conductivity was evaluated through the hot-wire apparatus. The hot-wire works on the principle of measuring the rising temperature of the probe. A digital viscometer was used to measure the viscosity characteristics of the base fluid, mono and hybrid nanofluids.

The consumed electric power of CNC lathe was recorded by a customized smart-meter through the main supply bus. Here, the total cutting power was measured while considering nine combinations of speed-feed in the experimental design. The direct cutting power was computed by deducting the spindle and feed power from the total power. The research methodology of the study is provided in Fig. 2.

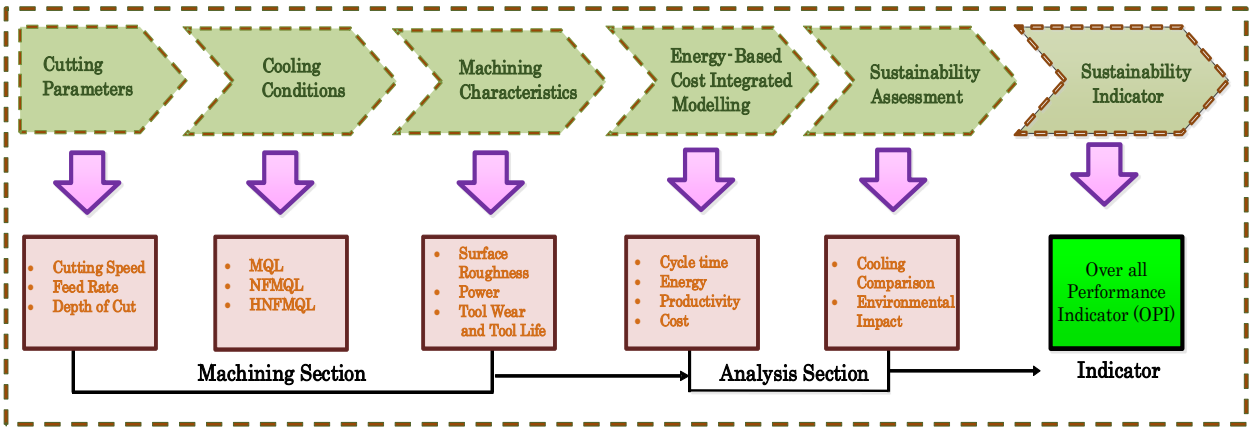

Fig. 2. Research methodology adopted in the present research work.

3.4 Preparation of mono and hybrid nanofluids

Alumina (Al_2O_3) is a cost-effective and widely used engineering ceramic material in the industry. It is demonstrated that tribological properties developed by the cutting fluids can be improved with the addition of graphene nanoparticles in base fluid (Lee et al., 2009).

A suspension with 25 vol.% concentration of Al_2O_3 nanoparticles (a spherical shape with a diameter of 45nm) in Ethylene glycol/DI-water and a colloidal suspension containing 18 vol.% concentration of graphene nano-platelets (mean particle size: 10-16 nm) was procured. The base fluid was obtained by mixing 15 vol.% concentration of Blaser cutting oil in DI. For the preparation of mono nanofluid (NFMQL), a 10% volumetric concentration of Al_2O_3 nanoparticles was mixed with the base fluid following the method proposed by (Devendiran and Amirtham, 2016). However, for the synthesis of alumina-graphene (Al-GnP), Al_2O_3 with graphene nano-platelets (GnP) was used with a ratio of 85:15 mixed in the base fluid at different concentrations (0.20%, 0.75% and 1.20% vol.). A Two-step method was applied to prepare hybrid (HNFMQL) cutting fluids (Sidik et al., 2014). An image with the nanoparticles in Al-GnP hybrid cutting fluid is displayed in Fig. 3. To ensure environmental safety, the nano-fluids were carefully filtered before being released to the sewer and a standard ventilator is used in the experimentation workplace to absorb the induced nano-mist in the surrounded air.

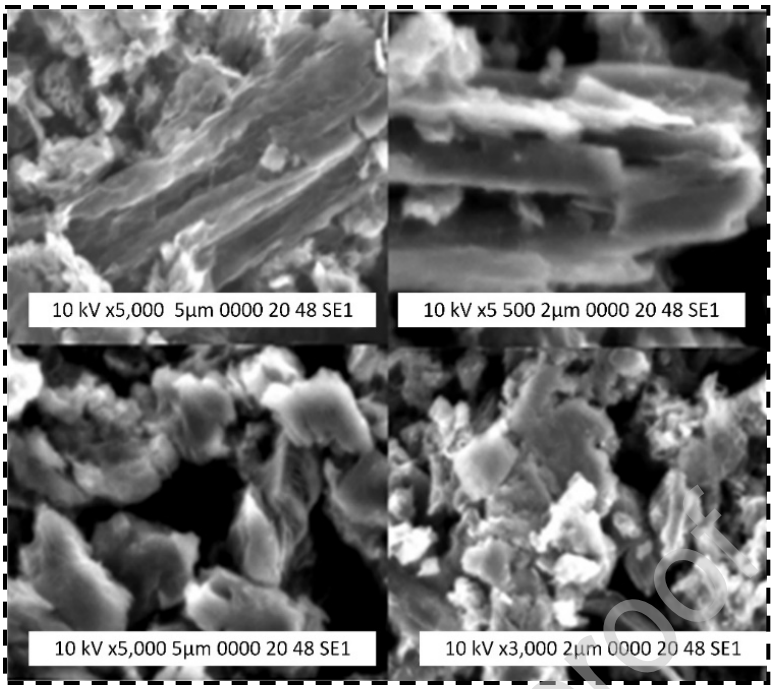

Fig. 3. Micrographs images of graphene nanoparticles

Each sample of nanofluid was kept in an ultrasonic cleaning machine (Equipment model: KQ-2200B, Frequency: 38 kHz, Power: 100 W) for over 6 hours to achieve a uniform suspension. A new nanofluid sample was prepared and used immediately to perform each experiment to avoid any sedimentation of nanoparticles.

4. Characterization of mono and hybrid nanofluids

Fig. 4 shows the effect of operating temperature on the thermal conductivity of the various synthesized nanofluids. At low temperature (~25°C), Al-GnP hybrid nanofluids showed 3.48% (vol.% 0.2), 7.44% (vol.% 0.7), and 9.03% (vol.% 1.2), improvement in thermal conductivity compared to base oil (MQL approach) (Mehrali et al., 2016). Hence, Al-GnP based hybrid nanofluid has a positive potential as a heat transfer fluid when used for high-speed machining. However, the thermal conductivity achieved for pure Al_2O_3 based nanofluid was higher than the conventional as well as hybrid.

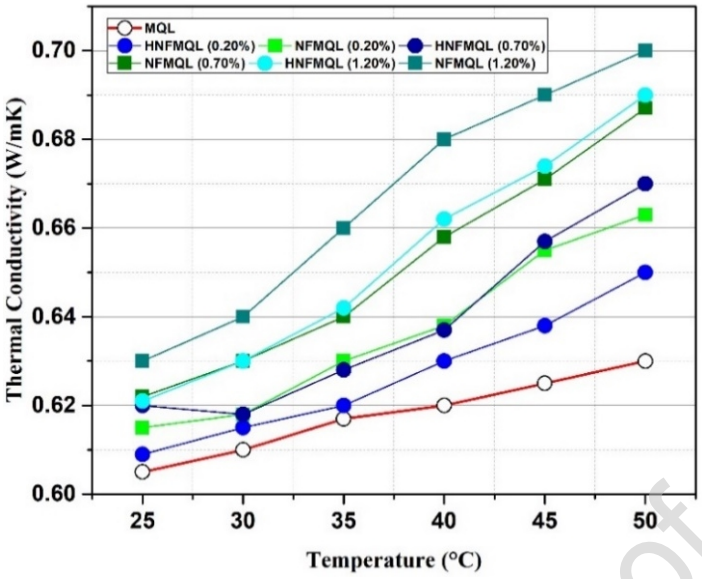

Fig. 4. Effect of increasing temperature on thermal conductivity of various types of fluids.

An implicit thermal conductivity may be obtained from summing up the cutting fluids' static and dynamic thermal conductivity. Moreover, the Brownian motion generated by the different nanoparticles is a well-known mechanism having a direct effect on thermal conductivity (Shukla and Dhir, 2008). The diffusion coefficient for Brownian motion is defined in Eq. (3).

$$D_b = {K_B T}/{3\mu\pi d_p} \qquad (3)$$

Here, D_b is the Brownian diffusion coefficient, T is temperature, K_B represents Boltzmann constant, μ denotes viscosity, d_P indicates nanoparticles' diameter. From Eq. (3), increasing viscosity results in a decrease in the Brownian diffusion coefficient (D_b). Similarly, a higher viscosity permits to decrease the nanofluids' thermal conductivity.

All types of fluids have shown the lower viscosity with increasing operating temperature. Fig. 5 indicates a 17.21%, 23.54%, and 39.24% increase in viscosity of Al-GnP at different concentration levels of 0.20%, 0.75%, and 1.20%, respectively, when compared with the classical MQL approach at room temperature.

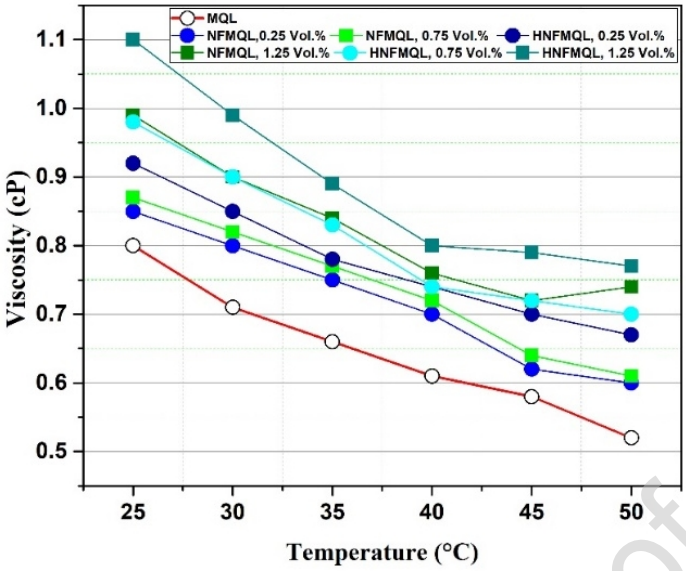

Fig. 5. Effect of temperature vs. viscosity of cutting fluids at different concentrations

From Fig. 4 and Fig. 5, it can be concluded that viscosity and thermal conductivity of the cutting fluids varied by increasing the temperature and nanoparticle concentration. The higher values of thermal conductivity have positive effects on the cutting zone when it is executed in the turning process. However, the increase in viscosity values creates a problem of pressure drop during NFMQL or HNFMQL spray. Thus, to obtain the most suitable nanofluids, the concentration of nanoparticles was varied from 0.20% to 1.20%. As a result, the synthesized hybrid cutting fluid showed a better lubrication property as compared to the base fluid.

Analysis of the Coefficient of Friction (CoF) in various nanofluid assisted turning process is a tedious job. Preliminary orthogonal cutting experiments were performed to analyze the CoF. Thrust force (F_t) and cutting force (F_c) were measured to find the CoF. The average CoF of the tool-chip interface can be found according to Eq. (4).

$$\mu = CoF = {}^{F_t}/_{F_c} \qquad (4)$$

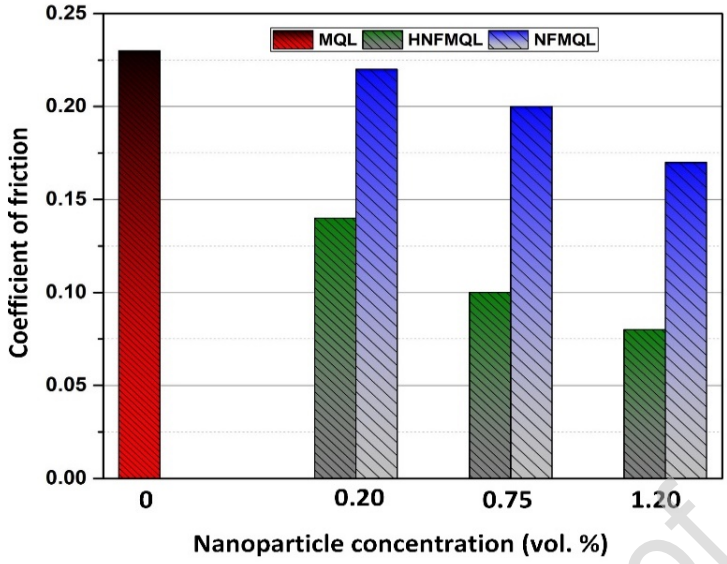

Fig. 6. Coefficient of friction of nanofluids and hybrid nanofluids under variation in nanoparticle concentration.

Fig. 6 indicates that higher nanoparticle concentration provides a lower value of CoF. This is due to the generation of a thin lubricating film, produced at the tool and chip interface. In addition, it can also be seen that at all concentration values of Al-GnP based cutting fluid yielded less CoF when compared with both the base fluid and Al_2O_3 based monotype nanofluid.

5. Modeling of Energy and Cost for Machining Process

5.1 Cycle time and energy consumption modeling

Traditionally, researchers estimate cutting power based on cutting force – shown in Eq. (5).

$$P_c = F_c \times v \tag{5}$$

where, P_c is cutting power, F_c is cutting force.

In the past, the Black-Box Approaches (BBA) were developed for modeling the energy consumption of a machine tool. In this manuscript, a Bottom-Up Approach (BUA) has been used to address the drawbacks of BBA. Cycle time (T_c) during the

turning of AISI 51200 hardened steel under advanced lubricooling approaches was divided into sub-components based on the different activities as defined in Eq. (6).

$$\text{Cycle time, } T_c = t_{sb} + t_a + t_c + t_{tc/p} \quad (6)$$

$$\text{Tool change time per part, } t_{ct/p} = {}^{t_{ct} \times t_c}/_{N \times T_L} \quad (6a)$$

$$\text{Tool change time per part, } t_c = {}^{\pi \times D \times l_c}/_{v_c \times f} \quad (6b)$$

$$\text{Standby time, } t_{sb} = t_{su} + t_i + t_h \quad (6c)$$

$$\text{Setup time, } t_{su} = t_{sut} + t_{suw} \quad (6d)$$

$$\text{Lubrication time, } t_{lub} = (0.5 \times t_a) + t_c \quad (6e)$$

where, t_{sb}, t_i, t_a, t_c, $t_{tc/p}$, t_{lub}, t_{su}, t_h, t_{sut}, t_{suw} are standby, idle, air cutting, cutting, tool change per part, lubrication, setup, handling, tool setup, and workpiece setup time, respectively. N is the total number of parts produced per parts, T_L is experimentally measured tool life, D is workpiece diameters and l_c is cutting length.

Therefore, by merging Equations (6a-6e) in Eq. (6), the cycle time per part can be determined as shown in Eq. (7):

$$T_c = t_{sb} + t_{lub} + {}^{1}/_{f}\left(l_a + l_c + {}^{t_{ct} \times l_c}/_{N \times T_L}\right) \quad (7)$$

where, l_a and l_c are air cutting, and cutting length, respectively.

The detailed profiles of cycle time, power and corresponding energy consumption during machining are portrayed in Fig. 7. The additional red line shows the power consumed by the air compressor.

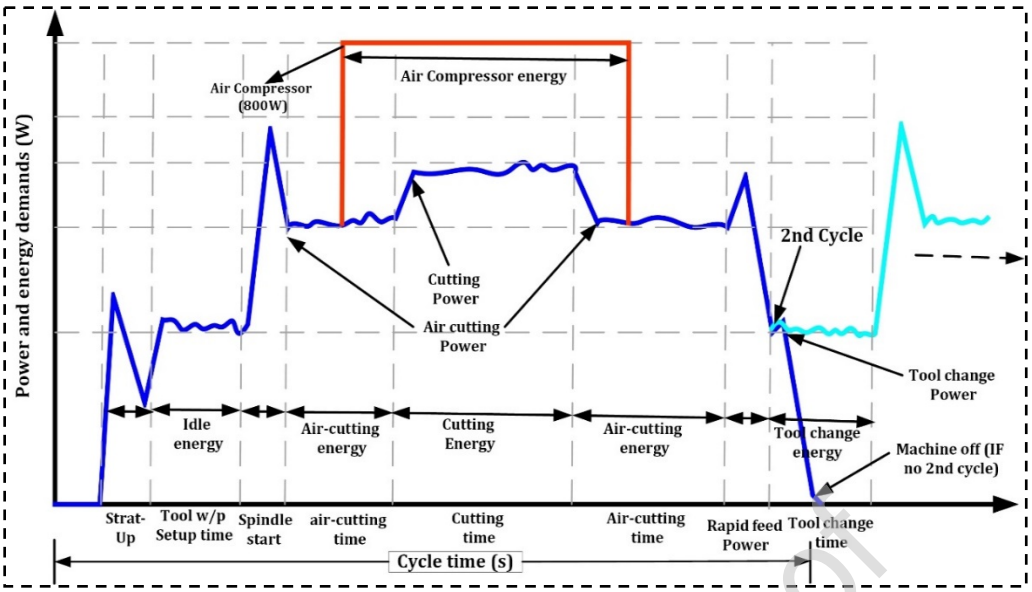

Fig. 7. Cycle time vs power along with energy consumption profiles of a machine tool to produce a machining routine.

Machine tool power consumption shows a significant change during the different functionality stages. The machine tool power during the idle/standby stage is P_{sb}, it is considered as a fixed power. Power due to spindle rotation (P_{spin}) can be calculated considering a virtually linear relationship with spindle rotation (Mativenga and Rajemi, 2011). Similarly, the operational power for the feed motor P_{feed} is calculated according to a linear relationship with feed-rate. The specific coefficients k_n, k_f, and b and c were used to calculate P_{spin}, and P_{feed} (Li et al., 2013). Cutting power was modeled by multiplying MRR with the specific cutting energy (k_0), following the procedure adopted in (Gutowski et al., 2006). Power used by the air compressor P_l was used in the MQL assisted cooling process. Eq. (8) shows the power consumption model.

$$P_t = P_{sb} + (k_n.n + b) + (k_f + f.n + c) + (k_0.MRR) + P_l \qquad (8)$$

The complex energy characteristics developed by the CNC is due to variation in the power consumption during different functionality stages. The BUA was applied to develop a new energy consumption model which is presented in Eq. (9).

$$EC = \int_0^{t_{sb}} P_{sb}(t)dt + \int_0^{t_a} P_a(t)dt + \int_0^{t_c} P_c(t)dt + \int_0^{t_{tc}} P_{tc}(t)dt + \int_0^{t_c} P_{lub}(t)dt \quad (9)$$

In Eq. (9), P_{sb}, P_a, P_c, and P_{tc}, and P_{lub} are power consumption during standby, air cutting, cutting tool change, and lubrication stages, respectively.

5.2 Cost modeling

The cost model presented in (Kalpakjian, Serope, 1995) has some limitations where it defines the total part cost as the sum of (1) machining cost (2) tool change (3) cutting-tool. However, the energy cost due to the non-cutting stage, lubrication stage, nanofluid preparation stage and environmental cost were not addressed. Furthermore, three groups of experiments were performed at the same cutting conditions to estimate the cost per part, shown in Eq. (10).

$$C_P = C_e + C_m + C_{CT} + C_f + C_{np} + C_{env} \quad (10)$$

Here, C_e represents the energy cost incurred due to the power consumption of machine tool, C_m represents machining cost, C_{CT} *is* cutting-tool cost, C_f is the fluid cost (base fluid, mono nanofluid and hybrid nanofluid) and C_{env} is the environmental cost.

$$C_e = X_e(P_i \times t_i + P_a \times t_a + P_c \times t_c + P_{tc} \times t_{tc/p} + P_{lub} \times (t_{lub} + 0.5 \times t_a) \quad (10a)$$

The unit cost of electricity is detonated by X_e.

Similarly, the machining cost $C_m = h_e \times (T_c)$ can also be achieved as follows:

$$C_m = h_e\left(t_i + t_{lub} + {}^{1}/_{f}\left(l_{air} + l_c + {}^{t_{ct} \times l_c}/_{N \times T_L}\right)\right) \quad (10b)$$

$$C_{CT} = X_{CT}\left({}^{t_c}/_{T_L}\right) \quad (10c)$$

$$C_f = X_f \times Q_F \times (t_c + 0.5 \times t_a) \quad (10d)$$

$$C_{env} = K_{CO_2} \times CE_P \quad (10e)$$

K_{CO_2} is the unit price of the environmental burden, CE_P represents total carbon emissions per part. In Eq. (10), X_e, X_{CT}, are per unit amount of cost of electricity, and cutting tool. The flow rate of various types of fluids in the MQL system is denoted by Q_F. Components of machining cost rate (h_e) and various components of cost modeling are shown in Appendix (A.1).

Putting Eq. (10a – 10e), in Eq. (10), we get a total part cost.

$$C_P = X_e \times (P_i \times t_i + P_a \times t_a + P_c \times t_c + P_{tc} \times t_{tc/p} + P_{lub} \times (t_{lub} + 0.5 \times t_a) + h_e \left(t_i + t_{lub} + {}^{1}/_{f}\left(l_a + l_c + {}^{t_{ct} \times l_c}/_{N \times T_L}\right)\right) + X_{CT}\left({}^{t_c}/_{T}\right) + X_{fluid} \times Q_F \times (t_c + 0.5 \times t_a) \quad (11)$$

Eq. (11) is a general expression for the cost estimation, however, for three different lubricooling environments, cost per part is shown in Equation (12-14).

$$C_{P/MQL} = X_e(P_i \times t_i + P_a \times t_a + P_c \times t_c + P_{tc} \times t_{tc/p} + P_{lub} \times (t_{lub} + 0.5 \times t_a) + h_e \times \left(t_i + t_{lub} + {}^{1}/_{f} \times \left(l_a + l_c + {}^{t_{ct} \times l_c}/_{N \times T_L}\right)\right) + X_{CT} \times \left({}^{t_c}/_{T}\right) + X_f \times Q_F \times (t_c + 0.5 \times t_a) \quad (12)$$

$$C_{P/NFMQL} = X_e(P_i \times t_i + P_a \times t_a + P_c \times t_c + P_{tc} \times t_{tc/p} + P_{lub} \times (t_{lub} + 0.5 \times t_a) \left(t_i + t_{lub} + {}^{1}/_{f}\left(l_a + l_c + {}^{t_{ct} \times l_c}/_{N \times T_L}\right)\right) + X_{CT} \times \left({}^{t_c}/_{T}\right) + X_{nf} \times Q_F \times + 0.5 \times t_a) \quad (13)$$

$$C_{P/HNFMQL} = X_e(P_i \times t_i + P_a \times t_a + P_c \times t_c + P_{tc} \times t_{tc/p} + P_{lub} \times (t_{lub} + 0.5 \times t_a) \left(t_i + t_{lub} + {}^{1}/_{f}\left(l_a + l_c + {}^{t_{ct} \times l_c}/_{N \times T_L}\right)\right) + X_{CT}\left({}^{t_c}/_{T}\right) + X_{hnf} \times Q_F \times + 0.5 \times t_a) \quad (14)$$

where, X_f, X_{nf} and X_{hnf} are per unit cost of the base fluid, monotype cutting fluid and hybrid cutting fluid, respectively.

6. Results and discussion

6.1 Surface quality and mechanism of nanoparticles

It is found that increasing the cutting speed decreases the surface roughness, this is commonly known in machining operations (Gupta et al., 2019; Khan et al., 2019b) (see Fig. 8). It is also observed that HNFMQL provides better results than both MQL and NFMQL at all cutting speeds. It should be stated that applying a nano-mist provides effective functions in terms of improving the cooling and lubrication properties during machining processes. Both mono NFMQL and hybrid HNFMQL nanofluids offer better tribological properties that promote an improved activity near the cutting tool and workpiece materials, and accordingly enhance the frictional behavior compared to the classical MQL.

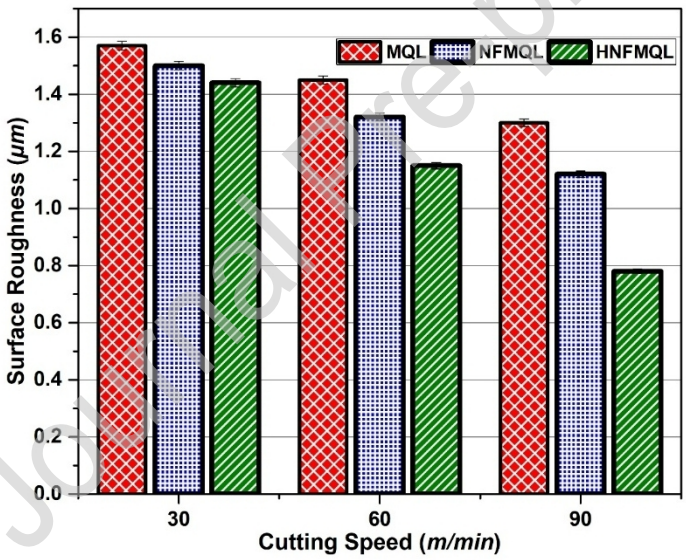

Fig. 8. Cutting speed effects associated to surface roughness (f = 0.1 mm/rev; n_p=0.7 (NFMQL and HNFMQL); a_p = 0.5 mm).

Fig. 9 demonstrates the effect of the percentage volume concentration of nanoparticle on the surface quality of workpiece. The results depict improved surface quality at 0.75 vol.% in comparison to the percentage volume concentration at 0.2 vol.%. However, a slight improvement was noticed at 1.25 vol.% as compared to 0.75

vol.%. Hence, increasing the nanoparticle volume percentage improves the overall heat transfer coefficient, and also offer less CoF.

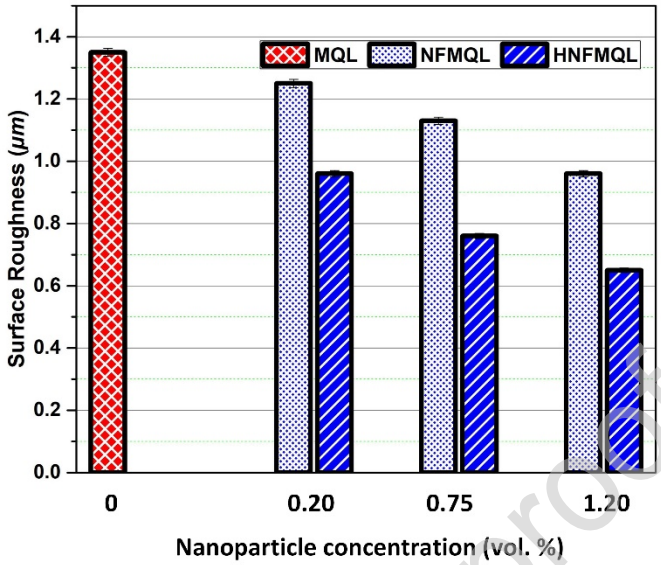

Fig. 9. Nanoparticles concentration-effect associated with surface roughness under different cooling approaches ($f = 0.1\ mm/rev$; $v_c = 90\ m/min$; $a_p = 0.5\ mm$).

Fig. 10 shows the improvements associated with applying NFMQL and HNFMQL through highlighting and showing their mechanisms. The mechanisms associated with these promising techniques can be divided into two main categories i.e., tribological and heat-transfer. The tribological mechanisms should be related to the "rolling effect" of the induced nano-mist. The rolling effect represents the presence of nano-additives in the cutting zone. The nano-additives act as rollers to decrease the resultant CoF which further reduces the rubbing severity (Eltaggaz et al., 2018). This significant effect has a vital role in improving tool-wear behavior as well as the induced surface quality.

In the heat-transfer mechanism, the dispersed nano-additives enhance the heat transfer performance in terms of the conduction and convective aspects. The application of nanofluids could lead to a formation of a very thin layer in the cutting-zone, this layer dissipates the generated heat from either the cutting tool or workpiece (Hegab et al., 2018).

In addition, the nano-mist presence in the cutting zone offers a conductive function to dissipate the generated heat. Thus, the severity of the cutting problems (e.g. plastic deformation, built-up-edge) associated with the high heat generation can be reduced.

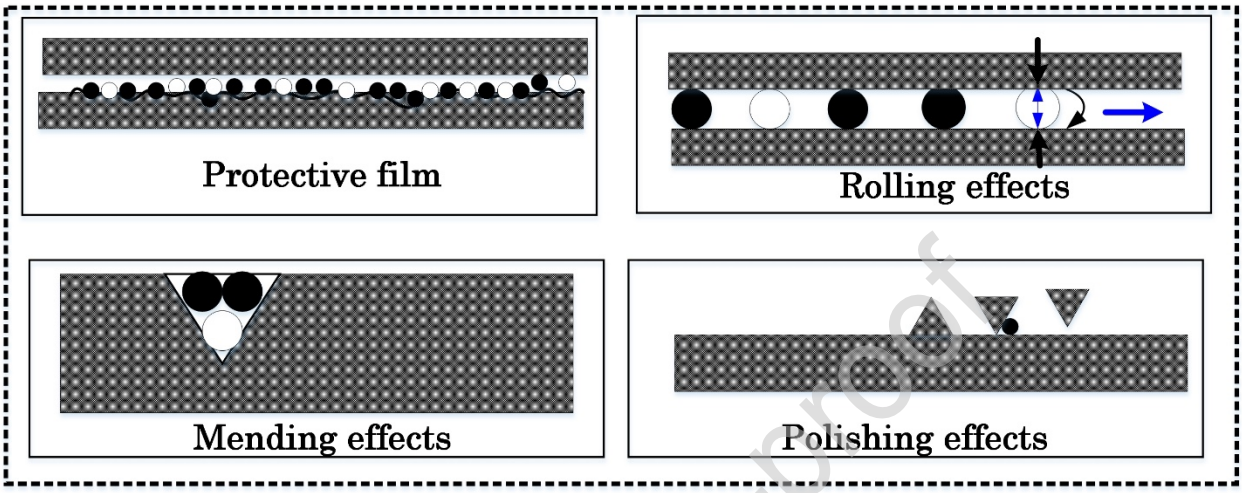

Fig. 10. Possible lubrication mechanisms of nano-fluids during turning AISI52100 (K. Lee et al., 2009)

6.2 Power and energy consumption

The section provides the details of the sustainable metrics i.e., cutting power, machine power, specific energy consumption, specific cutting energy and energy shares.

6.2.1 Cutting power and Machine power

It has been noticed that both the cutting power and machining power follows the increasing trend when the cutting speed values were increased from 30 to 90 m/min (Fig. 11). At higher cutting speeds, machine tool consumed more power due to which the cutting speed directly influenced the cutting power and machining power. In Fig. 11, the cutting power and machining power have higher values in the MQL cases followed by NFMQL and HNFMQL. Presumably, the same trend is observed at all cutting speed values. The least cutting power in HFMQL approach is because hybrid nanofluid produces less heat in the region of tool-chip interface and thereby, lower

cutting forces are required to plough the materials. Moreover, the hybrid nanoparticles produce more cushioning effect over the tool/chip interface and lower machining vibrations. Thus, it is worth mentioning that turning with HNFMQL conditions should be considered in a category of green and clean manufacturing.

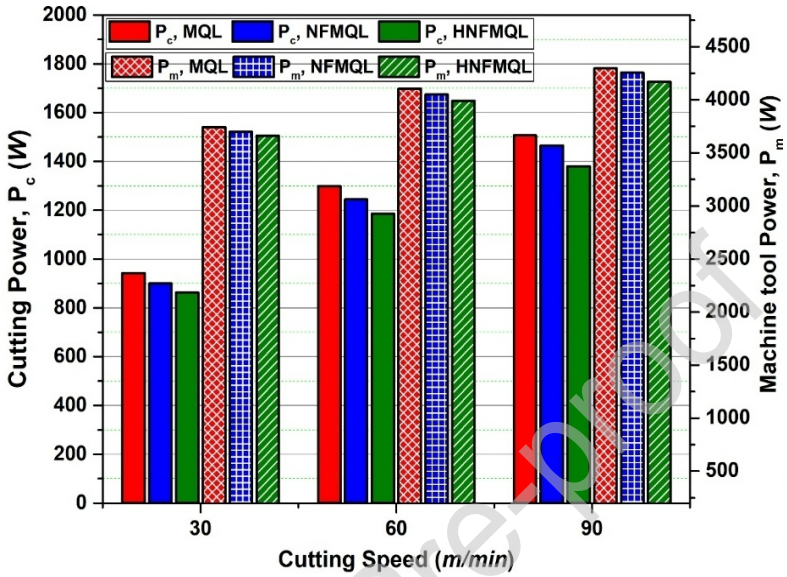

Fig. 11. Comparison of Cutting power and Machine power in MQL, NFMQL and HNFMQL cooling approaches with increasing cutting speed ($f = 0.1\ mm/rev$; $v_c = 90\ m/min$; $a_p = 0.5\ mm$).

Fig. 12 shows a comparison of cutting power and machine tool power values with respect to the variations of nanoparticle concentration. These results clearly demonstrate that the cutting power and machining power values are virtually the same at all concentrations of nanofluids. However, the cutting power is significantly lower at 1.20 vol.% in HNFMQL as compared to the conventional MQL approach. Thus, it can be observed that increasing nanoparticle concentration could lead to better frictional and heat transfer behavior. Increasing the nanoparticles concentration means that there are more nanoparticles in the tool-workpiece interface zone as discussed by (H. Hegab et al., 2018).

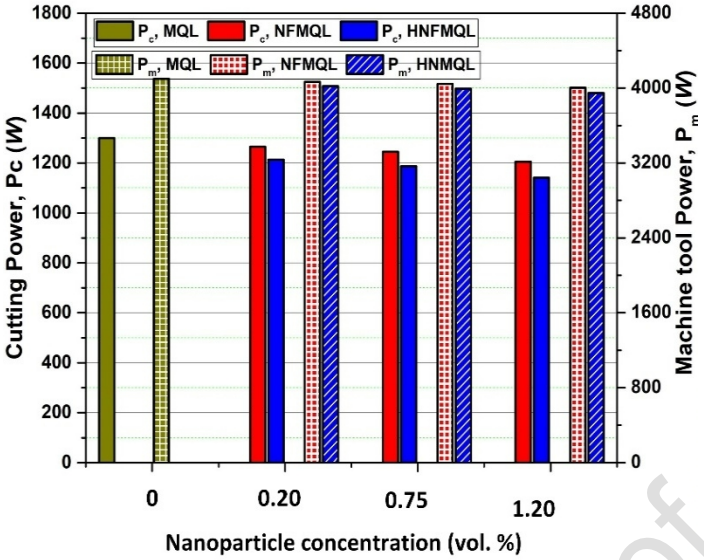

Fig. 12. Nanoparticles concentration vs. (Pc and Pm) in various cooling approaches ($f = 0.1\ mm/rev; v_c = 90\ m/min; a_p = 0.5\ mm$).

6.2.2 Specific energy consumption and specific cutting energy

The Specific Cutting Energy (SCE) represents the amount of energy used to cut out 1 mm^3 of material during metal cutting. However, SEC represents the total amount of energy used to cut out 1 mm^3 of workpiece material by all functionality states of the machine tool. That is why the SEC is many folds greater than SCE.

It can be seen from Fig. 13 that the increase in the nanoparticles concentration decreases the SCE. It is a fundamental principle of cutting mechanisms that the cutting forces and power consumption reduced as the CoF reduces (H. Hegab et al., 2018). It was observed that at vol.%=1.2, classical MQL consumes 2.2% and 1.7% more SCE as compared to mono NFQML and HNFMQL approaches, respectively. In contrast, the HNFMQL approach consumes 5.8% and 8.3% less SCE as compared to NFMQL and MQL approaches, respectively (Fig. 13).

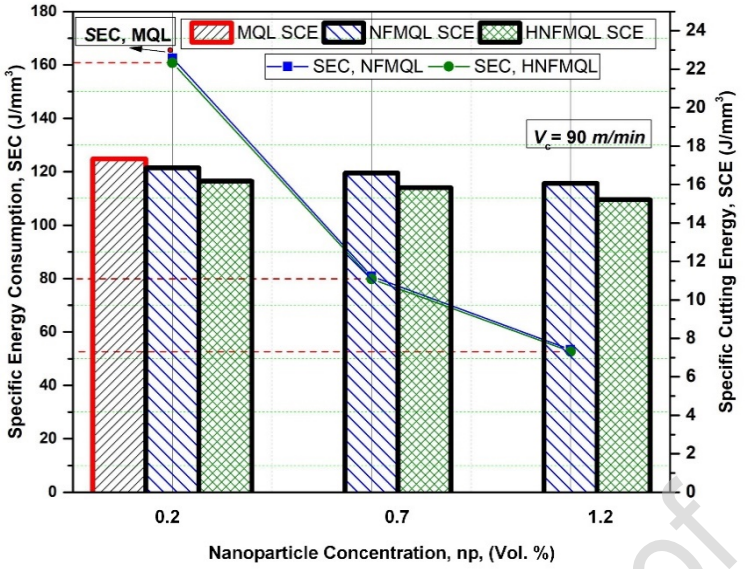

Fig. 13. Effect of nanoparticle Concentration on SEC and SCE values ($f = 0.1\ mm/rev; v_c = 90\ m/min; a_p = 0.5\ mm$).

It is evident from Fig. 14 that the SEC decreases significantly as the cutting speed increases. This happens due to the decrease in cycle time as the cutting speed increases (Li et al., 2017). When AISI 52100 steel is machined over MQL assisted machining, SEC decreased 45.16% and 58.66% by increasing the cutting speed from 30 m/min to 60 m/min and from 30 m/min to 90 m/min, respectively.

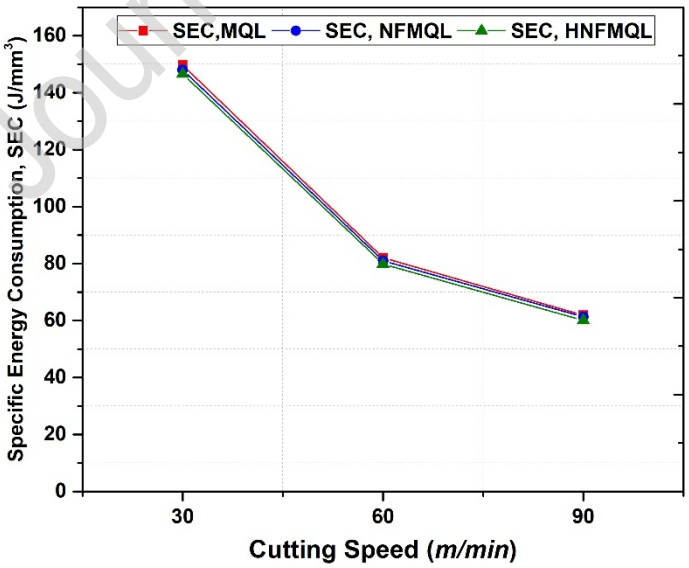

Fig. 14. Assessment of SEC w.r.t. increase in cutting speed in turning processes $(f = 0.1\ mm/rev; v_c = 90\ m/min; a_p = 0.5\ mm)$.

The higher cutting speed can massively reduce the tool lifespan when turning difficult-to-cut materials (Priarone et al., 2018). In addition, when the cutting tool life decreases, the tool change times (t_{tc}) increases and more electrical energy is consumed due to increased tool change time (Li et al., 2016). To sum up, the cutting speed is the most significant process parameters that affect the SEC. The benefit of the energy consumption model is also to provide energy-shares of each stage during the machining process. Fig. 15 graphically portrays the percentage contribution of each stage as total energy consumption in three different cooling approaches.

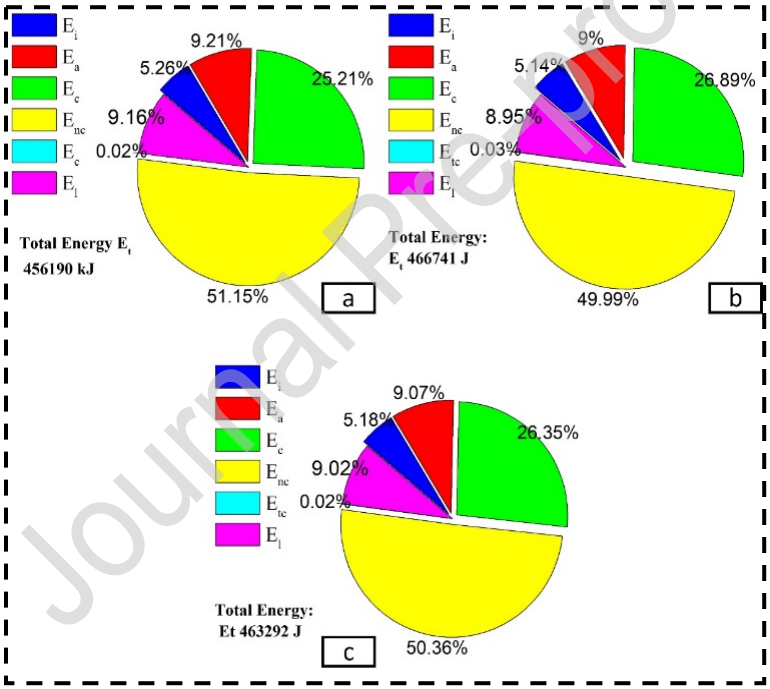

Fig. 15. Contribution of different machining stages in total energy consumption at $(f = 0.1\ mm/rev; v_c = 90\ m/min; a_p = 0.5\ mm)$.

In all three lubrication approaches, nearly half of the energy is consumed by non-machining functionality stages of the machine tool. In addition, 26.89%, 26.35%, and 25.89% energy is consumed due to cutting stages in MQL, NFMQL and HNFMQL, respectively. The sum of idle energy during standby time and tool change time was

nearly 5% of the total energy consumption in all machining approaches. The energy share provides new information for the machinist to identify and reduce energy consumption.

6.3 Tool wear and tool life

The spherical shape of the Al_2O_3 and 2D sheet structure of the graphene structure in a crystal plays an essential role in enhancing the performance of cutting fluids.

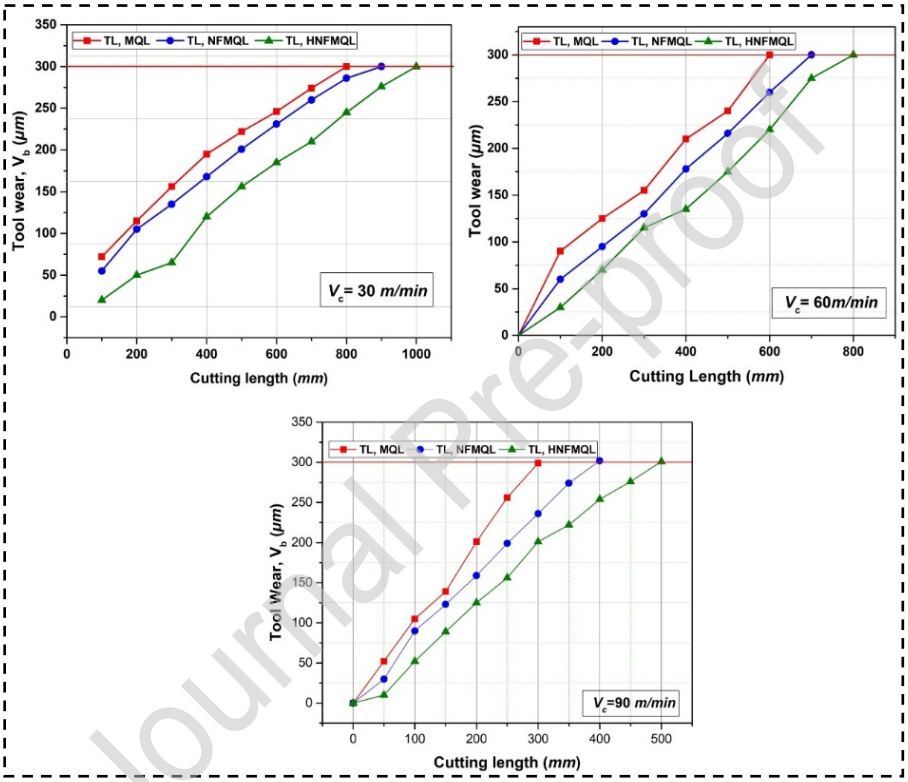

Fig. 16. Tool wear behavior for different cutting speeds during turning (f is set at 0.1 mm/rev; n_p is 0.7; a_p is 0.5 mm). ($f = 0.1\frac{mm}{rev}$; $n_p = 0.7$; $a_p = 0.5\,mm$).

Higher cutting speed may generate a large amount of tool wear. HNFMQL offers better tool-wear behavior at all cutting speeds compared to the MQL, and even NFMQL (Fig. 16). The applied nano-mist offers better heat transfer coefficient than the MQL, and accordingly decreases the extensive induced heat from the cutting operation. These effects are responsible for achieving a reasonable thermal softening

and decrease the induced cutting forces. From Fig. 16, it was noted that HNFMQL assisted machining produced more cutting-tool life in terms of cutting length.

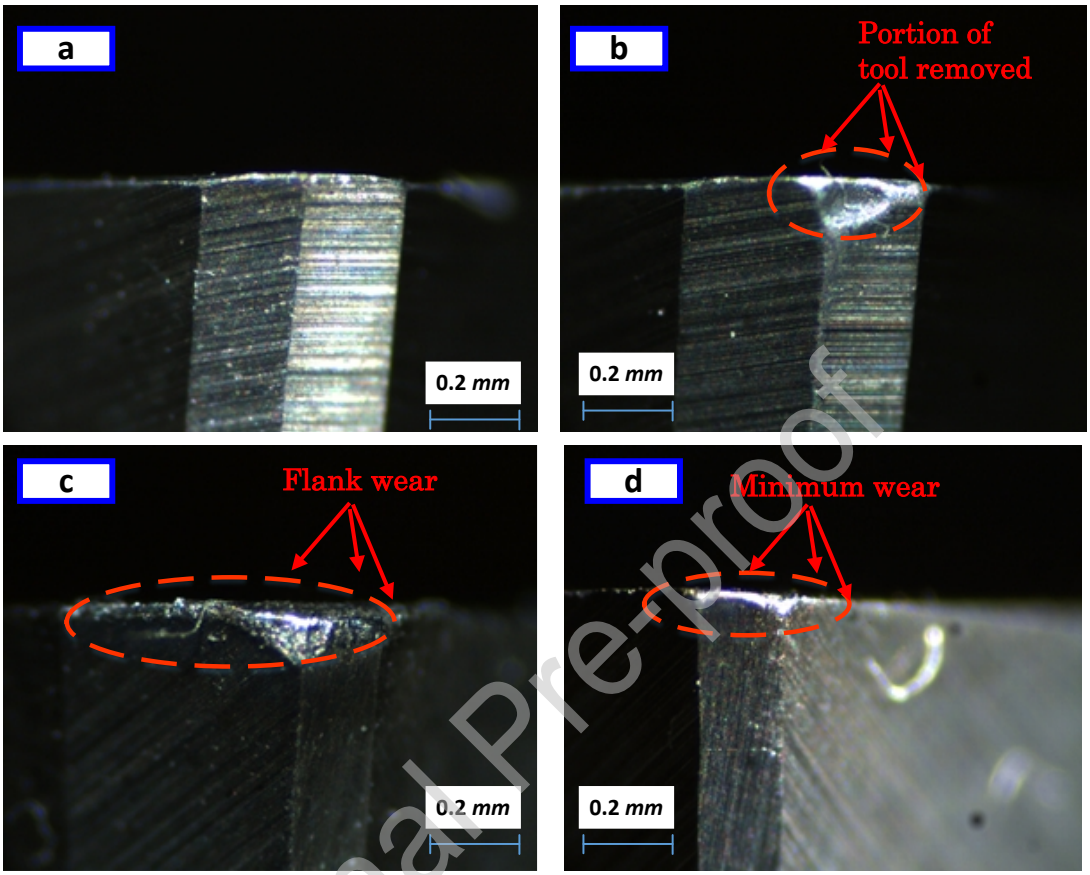

Fig. 17. Wear at flank side of cutting tool at $(f = 0.1\frac{mm}{rev}; v_c = 90\frac{m}{min}; n_p = 0.7;\ a_p = 0.5\ mm)$ (a) New tool (b) MQL (c) NFMQL (d)HNFMQL

In addition, the tool wear mechanisms (see Fig. 17 & 18) confirm the same findings obtained in Fig. 16 as both NFMQL and HNFMQL approaches offer better tool wear performance than the MQL. Compared with MQL, lesser flank-wear was observed when hybrid nanofluids were applied at cutting zone, (see Fig. 17-b). In MQL, this phenomenon may be attributed to a hybrid mechanism that consists of adhesive and abrasive wear (Eltaggaz et al., 2018). The reason for less flank wear in HNFMQL assisted machining process is associated with the weak Vander wall forces (Dai et al., 2016). During the cutting process, shear action takes place which exfoliates the weak sheet-structure of GnP and this phenomenon leads to the

formation of a tribo-film. The thin tribo-film enables the lubrication process that leads to lower CoF. The film thickness performance may be improved by a higher nanoparticle concentration.

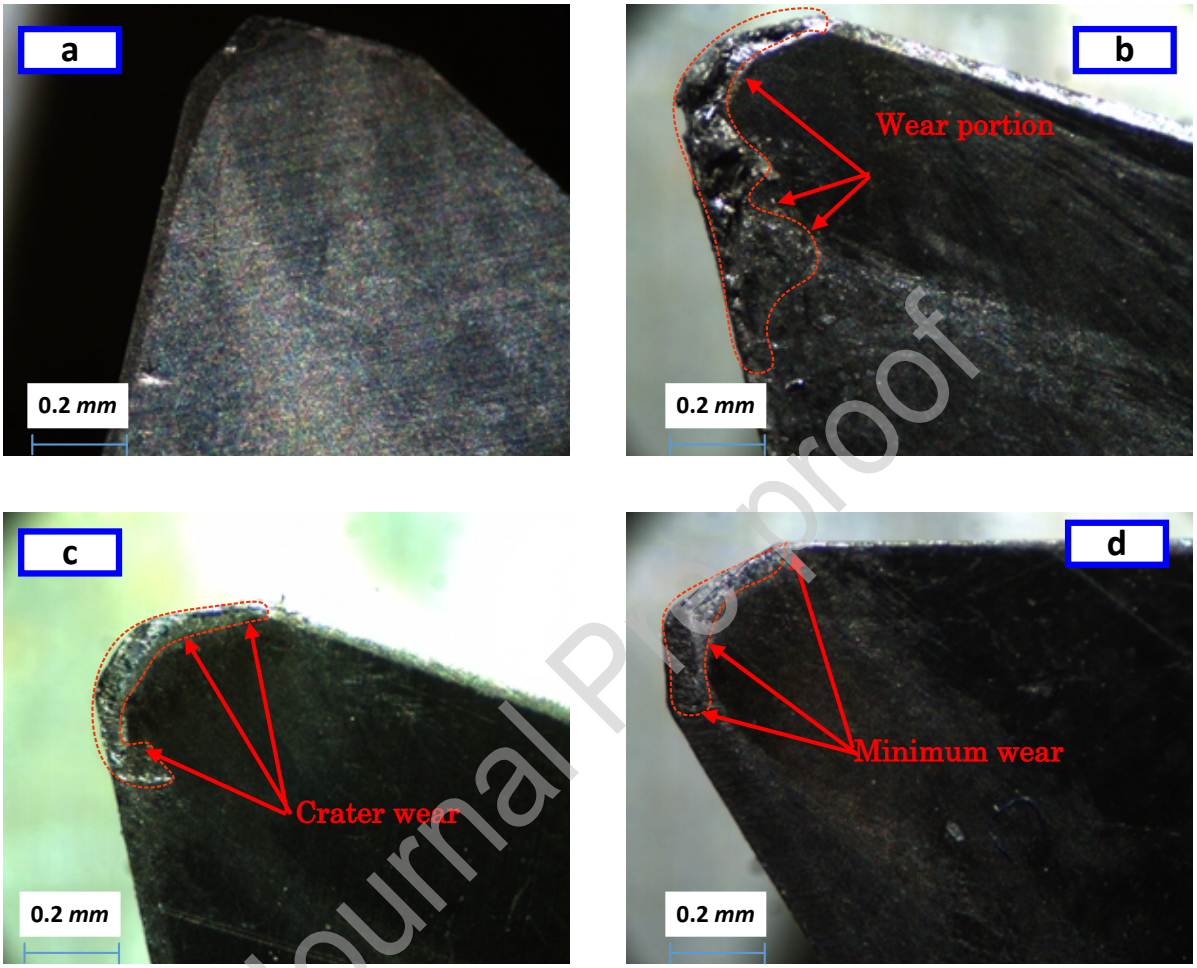

Fig.18. Wear at rake face: Crater wear at $(f = 0.1\frac{mm}{rev}; v_c = 90\frac{m}{min}; n_p = 0.7;\ a_p = 0.5\ mm)$ (a) New tool (b) MQL (c) NFMQL (d)HNFMQL

The adhesion is caused mainly by higher contact pressure produced at the tool and workpiece interfaces under high cutting temperatures (Gupta et al., 2019). Regarding the abrasive mechanism, it is mainly due to the hard elements in the workpiece material. Fig. 17-c and Fig. 17-d prove that hybrid (Al-GnP) nanofluids offer better performance with respect to mono (Al_2O_3) nanofluids. We suspect that the

hybrid nano-mist provides higher heat transfer capacity which enhances the cooling properties, and accordingly improves the interface bonding at the tool-workpiece zone.

While using the MQL, severe crater wear occurred because of the high generated heat (Fig. 18). It was also noted that, in both NFMQL and HNFMQL assisted machining of hardened AISI 52100 steel, initially the cutting-tool wears quickly, however the rate of wear becomes steady after a certain time. This was attributed to the development of tribo-film, once it is developed, cutting-tool wear rate stabilizes.

6.4 Productivity under advanced MQL approaches

Fig. 19 illustrates the comparison of the material removal volume (V) of a cutting-tool in machining under three lubrication approaches. It is noted that the increase in the MRV is associated with higher cutting speed (Khan et al., 2019a).

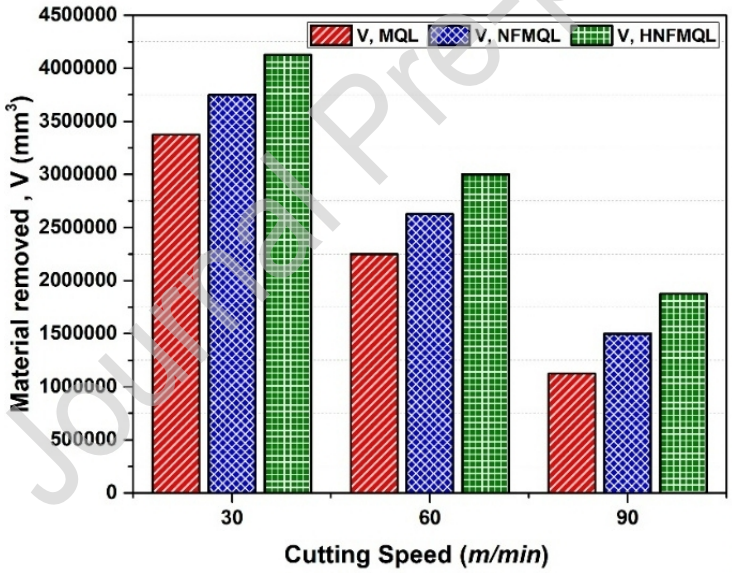

Fig. 19. Productivity-based comparison of various cooling approaches using different cutting speed ($f = 0.1\frac{mm}{rev}; n_p = 0.7; a_p = 0.5\,mm$).

At 90 m/min, the cutting-tool life in MQL, NFMQL, and HNFMQL approaches are 4.2, 5.6 and 6.9 minutes, respectively. The cutting tool lifespan decreases at higher cutting speed, therefore the MRV decreases. It can be said that higher cutting speeds are suitable for minimizing the SEC, but it will reduce the MRV per cutting

tool. Nearly 50% more MRV is removed at 30 m/min as compared to 90 m/min. An interesting situation arises for the decision-makers and practitioners to decide an optimal cutting speed that is suitable for the less energy and high MRV per cutting tool.

6.5 Machining cost

Production cost mainly depends upon the system boundaries of the machining process. Moreover, production cost (C_P) highly depends upon the number of resources (components) used and functionality stages of machine-tool. In this study, the focus was to compare the cost of three sustainable lubrication approaches. Therefore, the workpiece material cost was not included in the cost models in Eqns. (12-14).

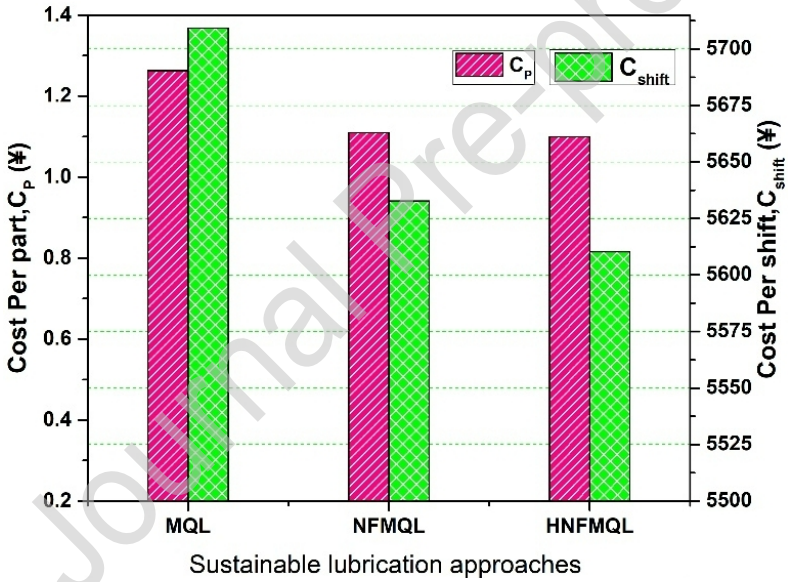

Fig. 20. Cost estimation per part (C_p) and compassion between various sustainable cooling approach at (f is 0.1 mm/rev; v_c is 90 m/min; n_p is 0.7; a_p is 0.5 mm).

For comparison, the main difference between the three approaches is the application of nanoparticles. In the MQL approach there are no nanoparticles, so it should be cheaper. However, it can be seen from Fig. 20, HNFMQL produces 0.4% and 1.7% lower-priced parts as compared to NFMQL and MQL approaches, respectively. The reduced price per part in the HNFMQL approach is due to larger

cutting-tool life at the same cutting conditions as that of MQL and NFMQL approaches. It is essential to reveal that a part is defined as one pass with a 50 mm cut in length. Data per shift was collected from Nanjing Dongmo Electromechanical Manufacturing Co., Ltd.; a local manufacturing company in China. A total of 5068 parts were produced per shift under each lubrication approach. HNFMQL assisted turning can save 98.98 ¥ per shift (shift with 20% downtime) as compared to the MQL approach.

7. Comparison of advanced - MQL Approaches: Performance and Sustainability Assessment

In this section, a comparison is established to discuss the effectiveness of the three used MQL approaches from sustainability perspectives. This assessment is closely related to results gathered in previous sections. In this assessment, equal weightage is assigned for each metric i.e., surface roughness, Power and energy consumption, tool life, MRV, production cost. In addition, the waste-management component was added as a qualitative metric in order to effectively assess the three studied strategies. A summarized flow chart for the applied algorithm used to assess the three studied approaches is provided in Fig. 21 (Hegab et al (b), 2018).

The main steps include the determination of the studied indicators, normalization, weighting, and determining the Overall Performance Index (OPI) for each lubricooling approach. The waste management factor was considered as "lower-the-better" factor. For the HNFMQL approach, the waste management factor was assigned as 3, while it was 2 for the NFMQL approach, and was 1 for MQL approach. Another factor of environment and health was also added in the proposed algorithm. This effect had the same criteria as the waste management factor, a value of 2 was assumed to both NFMQL and HNFMQL, and a value of 1 was assigned to the MQL approach.

The mathematical formulation for the assessment algorithm is achieved using Eqns. (15 &16), where PI is normalized Performance Index for each approach per

studied indicator, AP is Actual Performance achieved by each lubrication approach and OP is the Optimal Performance, n denotes the studied indicator number.

$$\begin{cases} \mathrm{PI} = \dfrac{\mathrm{AP}}{\mathrm{OP}} \text{ if sustainable indicator is based on} \\ \text{higher} - \text{the} - \text{better criteria (Higher the Better)} \\ \mathrm{PI} = \dfrac{\mathrm{OP}}{\mathrm{AP}} \text{if the sustainable indicator is not Higher the Better} \end{cases} \tag{15}$$

$$\mathrm{OPI} = \frac{\sum_{i=1}^{n} \mathrm{PI_i}}{n} \tag{16}$$

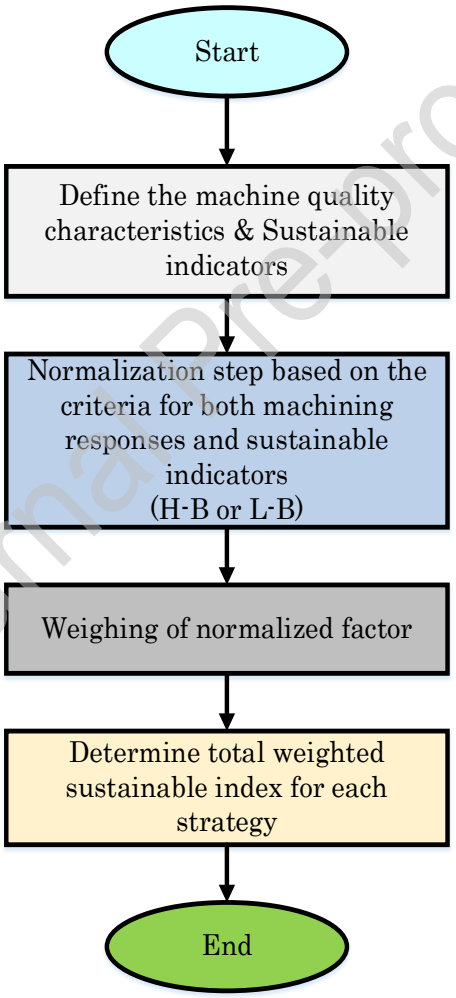

Fig. 21. The assessment steps for an overall evaluation.

Table 2. Sustainability assessment procedure

Assessment Indicators	Criteria	Cutting Conditions	Response Values			Performance Index (PI)			Weighted Performance Index		
			MQL	NFMQL	HFNMQL	MQL	NFMQL	HFNMQL	MQL	NFMQL	HFNMQL
Surface roughness results (μm)	lower-the-better	1: v_c=30 m/min	1.58	1.5	1.43	0.91	0.95	1	0.0430552	0.0453514	0.0475714
		2: v_c=60 m/min	1.45	1.31	1.16	0.8	0.89	1	0.0380571	0.0421243	0.0475714
		3: v_c=90 m/min	1.3	1.15	0.78	0.6	0.68	1	0.0285429	0.0322658	0.0475714
Cutting power results (Watt)	lower-the-better	1: v_c=30 m/min	940	900	865	0.9202128	0.96	1	0.0437758	0.0457214	0.0475714
		2: v_c=60 m/min	1300	1240	1195	0.92	0.96	1	0.0437291	0.045845	0.0475714
		3: v_c=90 m/min	1510	1475	1390	0.92	0.94	1	0.0437909	0.04483	0.0475714
Cutting length (mm) at tool wear of 0.3 mm	higher-the-better	1: v_c=30 m/min	800	890	1000	0.8	0.89	1	0.0380571	0.0423386	0.0475714
		2: v_c=60 m/min	600	690	800	0.75	0.86	1	0.0356786	0.0410304	0.0475714
		3: v_c=90 m/min	300	400	500	0.6	0.8	1	0.0285429	0.0380571	0.0475714
Volume of material removed (mm^3)	higher-the-better	1: v_c=30 m/min	3300000	3750000	4150000	0.80	0.90	1	0.0378279	0.0429862	0.0475714
		2: v_c=60 m/min	2250000	2600000	3000000	0.75	0.87	1	0.0356786	0.0412286	0.0475714
		3: v_c=90 m/min	1150000	1500000	1800000	0.64	0.83	1	0.0303929	0.0396429	0.0475714
Cost per part ($)	lower-the-better	1: v_c=30 m/min 2: v_c=60 m/min 3: v_c=90 m/min	1.125	1.11	1.1	0.99	0.99	1	0.1409524	0.1415701	0.1428571
Waste management	lower-the-better		1	2	3	1	0.5	0.33	0.1428571	0.0714286	0.047619
Environmental and health effect	lower-the-better		1	2	2	1	0.5	0.5	0.1428571	0.0714286	0.0714286
Overall Performance Index (OPI)									**0.87**	**0.79**	**0.83**

The assessment results are provided in Fig. 22 and in Table 2. Assessment indicators are shown in the first column of the table and their desired values are depicted in front of them. The PI was calculated from response values using Eq. 15. Lastly, the OPI was obtained from performance indices using Eq. 16.

It should be stated that the OPI or the total weighted sustainable index is based on "higher-the-better" criteria. It is found that MQL showed the highest OPI of 0.87 whereas slightly lower OPIs are obtained for NFMQL and HNFMQL approaches due to the difficult preparation procedures and hazardous nature of nanofluids. Applying adequate safety and environmental procedure as well as following standard instructions for waste management can compensate for this slight effect. Thus, these results can still confirm the competitiveness of using an advanced HNFMQL approach with the MQL.

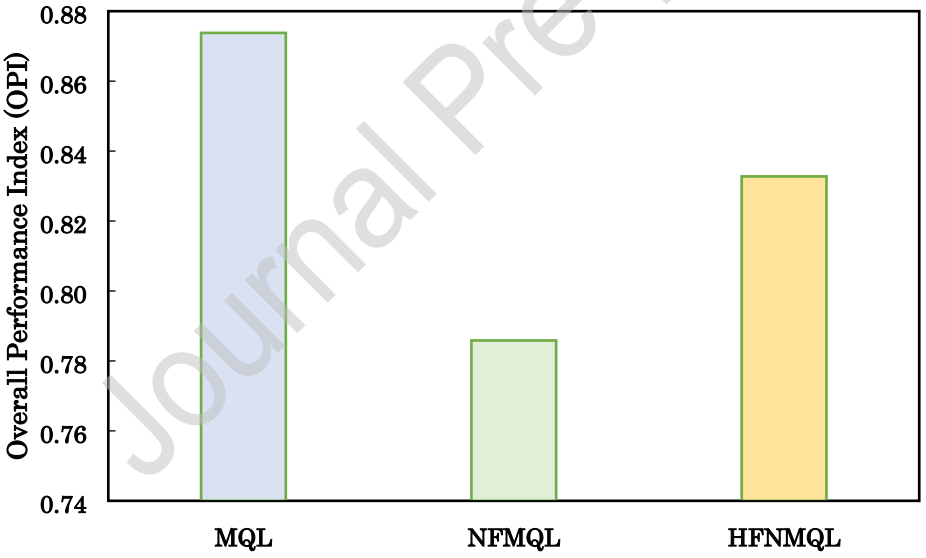

Fig. 22. The overall assessment results for MQL, NFMQL and HNFMQL approach.

8. Calculation of carbon emission signatures (CES)

Carbon emissions during the machining stage usually mimic the behavior of electrical energy consumption. In local power grids, during the combustion process, carbon emission is an inevitable consequence of electricity generation. Coal, oil, gas

and biomass are four prominent used fossil fuels. Information related to enthalpy and the chemical reaction of the combustion process is given below in Table 3.

Table 3. Energy produced by various types of fuels

No.	Type of fuel	1 GJ of heat produced	Release ΔH (kJ)	Release CO_2
1	Biomass	$CH_2O + O_2 \rightarrow CO_2 + H_2O$	−440	100 kg
2	Heavy oil	$C_{20}H_{42} + 30O_2 \rightarrow 20CO_2 + 21H_2O$	−13300	66 kg
3	Coal	$C + O_2 \rightarrow CO_2$	−394	112 kg
4	Natural gas	$CH_4 + 2O_2 \rightarrow CO_2 + 2H_2O$	−440	49 kg

$\Delta H = Enthalphy$

Coal consumption for power generation is responsible for the highest amount of carbon emission. It is important to understand that for every gigajoule of energy released, there is a certain amount of CO_2 emissions associated with it which depends upon the type of fuel used (Fig. 23).

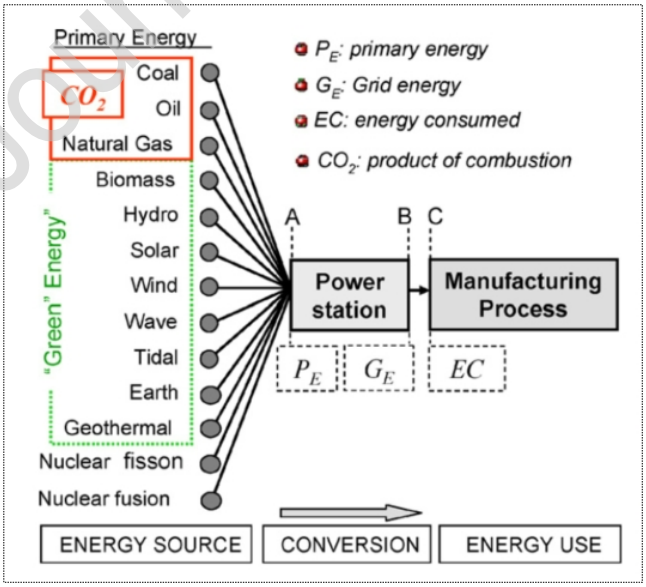

Fig. 23. Various sources of primary energy (Jeswiet and Kara, 2008).

Power supply grids for three jurisdictions and their type of fuel used is shown in Table 4.

Table 4. Three power grids of different countries and their input fuel type.

Fuel supply	Ontario (%)	NSW (%)	**Nanjing**
Coal (C)	19	83.9	73.09
Natural Gas (NG)	7	8.5	12.1
Petroleum (P)	0	0.3	0
Biomass (B)			
Solar (S)	23	7.3	
Hydropower (H)			0.09
Solar (S)			0
Solar (S)			6.92
Wind (W)			5.96
Geothermal (G)			
Earth (E)			
Wave (Wa)			
Tidal (T)			
Nuclear (N)	51		1.8
Total	**100**	**100**	**100**

The total carbon emitted in the process can be obtained by total energy consumption multiplied by carbon emission signature.

$$CE = E_{total} \times CES \tag{17}$$

Each electric grid possesses a Carbon Emission Signature (CES). It is necessary to find the CES of the Nanjing power grid that supplies electricity to an advanced cutting laboratory where experiments were conducted. The percentage values of Table 4 will become the coefficient of the equation used to calculate CES (Jeswiet and Kara, 2008).

$$CES = \eta \times (112 \times \%C + 49 \times NG + 66 \times \%P) \tag{18}$$

The carbon emission per part due to electrical energy consumption can be calculated as follow.

$$CE_{m/p} = E_{m/p}(J) \times CES(kgCO_2/J) \quad (19)$$

A holistic comparison including 15 metrics has been performed (Fig. 24). The environmental cost ($0.40\ ¥/kg$) has been imposed on the total carbon emission. As, MQL, NFMQL and HNFMQL approach use the minimal amount of oils and water thus there need for part cleaning, recycling and disposal is minimal.

Cutting tool life, the material removed, and operator health are required higher-the-better and all remaining metrics must be at lower values. The application of hybrid nanoparticles can not only reduce production cost and CO_2 emission but also significantly improve surface quality. Overall, HNFMQL assisted process has performed better as compared to MQL and NFMQL approaches (referred to Fig. 24 and **Appendix A.2**).

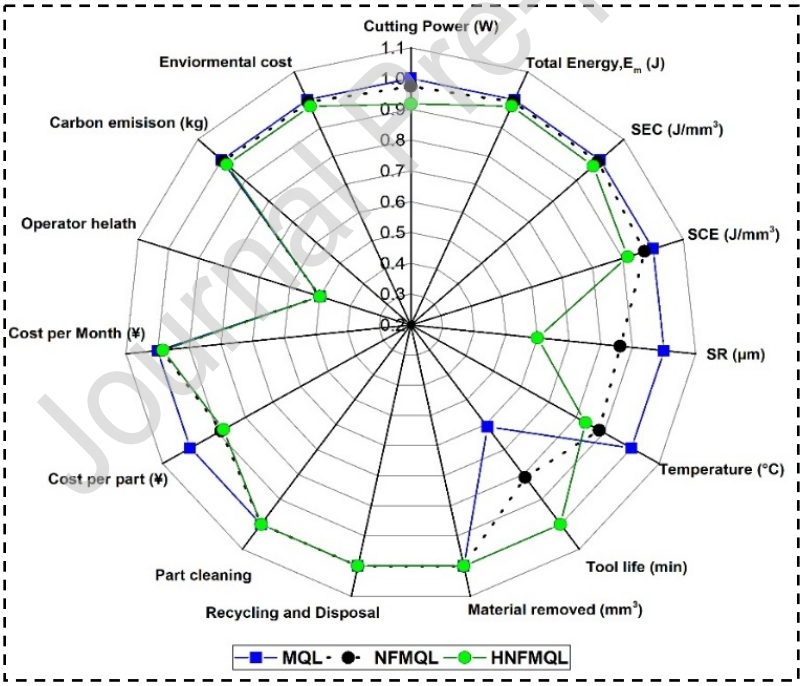

Fig. 24. Overall performance comparison of advanced-MQL assisted machining process ($f = 0.1\frac{mm}{rev}$; $v_c = 90\frac{m}{min}$; $a_p = 0.5\ mm$; $n_p = 0.7$).

9. Conclusion

The performance of the HNFMQL approach in the turning of hardened steel was evaluated in comparison to MQL and NFMQL. Empirical models were developed and machining metrics such as, surface quality, cutting power, SCE, SEC, MRV, tool life and production cost were measured and compared. In addition, the energy-integrated heuristic algorithm for sustainable machining was developed and discussed. After analyzing the experimental results, the main implications were summarized as follows,

- The surface quality of the workpiece was significantly improved with the use of HNFMQL assisted machining process.
- Both cutting power and machining tool power increased with the increase of cutting speed in all lubrication approaches. However, HNFMQL assisted machining consumed less cutting power at all cutting speeds.
- At all cutting conditions, HNFMQL assisted hard turning consumed less SEC and SCE when compared with MQL and NFMQL approach. At constant cutting speed, SEC reduced to 50% at (vol.%= 0.7) as compared to initial value of (vol.%= 0.2). The contribution of cutting energy was one-fourth of the total electrical energy consumed by the machine tool.
- For tool life analysis, the application of HNFMQL approach not only enhanced the tool life but also maximized the MRV per tool life. The cost per part produced by the HNFMQL approach was 0.4% and 1.7% less as compared to NFMQL and MQL respectively.
- OPI is a novel indicator that shows the overall sustainability of a machining process. The OPI of the proposed method can be further increased by improving waste management and environmental health and safety indicators.
- The novel results preach industry to implement the proposed sustainable approach to enhance the overall machining performance, consequently replacing the conventional MQL with HNFMQL approach.

Future Directions

The limitation of the study is that the proposed holistic model doesn't include the energy-cost assessment of the parts inventory. The impacts of cutting fluid on the health and safety of workers need to be elaborated. In addition, advance heuristic algorithm-based optimization of the cutting parameters for achieving the optimal sustainable metrics can be performed in the future.

Acknowledgment

The paper is one of the jewels of the PhD research work of the first author. The authors want to thank the editor and the anonymous reviewers as their comments helped us improve the quality of the paper. The authors are also thankful to Mr. Fawad Ahmad from Riga Technical University, Latvia for his valuable suggestions to improve manuscript.

Funding

The work is supported by the National Key Research and Development Project (2018YFB2002202) and [Grant No. U1601204]. The authors are also grateful to the National Natural Science Foundation of China (no. 51922066), the Major projects of National Science and Technology (Grant No. 2019ZX04001031), the National Science Outstanding Youth Fund of Shandong Province (Grant No. ZR2019JQ19). The authors declare that there is no conflict of interest.

References

Abdul Sani, A.S., Rahim, E.A., Sharif, S., Sasahara, H., 2019. Machining performance of vegetable oil with phosphonium- and ammonium-based ionic liquids via MQL technique. J. Clean. Prod. 209, 947–964. https://doi.org/10.1016/j.jclepro.2018.10.317

Bagaber, S.A., Yusoff, A.R., 2019. Energy and cost integration for multi-objective optimisation in a sustainable turning process. Meas. J. Int. Meas. Confed. 136, 795–810. https://doi.org/10.1016/j.measurement.2018.12.096

Cabanettes, F., Faverjon, P., Sova, A., Dumont, F., Rech, J., 2017. MQL machining: from mist generation to tribological behavior of different oils. 90, 1119-1130. Int. J. Adv. Manuf. Technol. https://doi.org/10.1007/s00170-016-9436-0

Campitelli, A., Cristóbal, J., Fischer, J., Becker, B., Schebek, L., 2019. Resource efficiency analysis of lubricating strategies for machining processes using life cycle assessment methodology. J. Clean. Prod. 222, 464–475. https://doi.org/10.1016/j.jclepro.2019.03.073

Dai, W., Kheireddin, B., Gao, H., Liang, H., 2016. Roles of nanoparticles in oil lubrication. 102, 88-98. Tribol. Int. https://doi.org/10.1016/j.triboint.2016.05.020

Devendiran, D.K., Amirtham, V.A., 2016. A review on preparation, characterization, properties and applications of nanofluids. Renew. Sustain. Energy Rev. https://doi.org/10.1016/j.rser.2016.01.055

EIA, 2013. International Energy Outlook 2013 US Energy Inf. Adminis- tration 312.

Eltaggaz, A., Hegab, H., Deiab, I., Kishawy, H.A., 2018. Hybrid nano-fluid-minimum quantity lubrication strategy for machining austempered ductile iron (ADI). Int. J. Interact. Des. Manuf. 12, 1273–1281. https://doi.org/10.1007/s12008-018-0491-7

Filipovic, A., Stephenson, D.A., 2006. Minimum Quantity Lubrication (MQL) applications in automotive power-train machining. 10, 3-22. Mach. Sci. Technol. https://doi.org/10.1080/10910340500534258

Gupta, M.K., Mia, M., Singh, G.R., Pimenov, D.Y., Sarikaya, M., Sharma, V.S., 2019. Hybrid cooling-lubrication strategies to improve surface topography and tool wear in sustainable turning of Al 7075-T6 alloy. Int. J. Adv. Manuf. Technol. 101, 55–69. https://doi.org/10.1007/s00170-018-2870-4

Gupta, M.K., Sood, P.K., Sharma, V.S., 2016. Optimization of machining parameters and cutting fluids during nano-fluid based minimum quantity lubrication turning of titanium alloy by using evolutionary techniques. J. Clean. Prod. 135, 1276–1288. https://doi.org/10.1016/j.jclepro.2016.06.184

Gutowski, T., Dahmus, J., Thiriez, A., 2006. Electrical Energy Requirements for Manufacturing Processes, in: 13th CIRP International Conference on Life Cycle Engineering, (Vol. 31, No. 1, pp. 623-638), Belgium,Leuven.

Hegab, H., Umer, U., Deiab, I., Kishawy, H., 2018. Performance evaluation of Ti–6Al–4V machining using nano-cutting fluids under minimum quantity lubrication. Int. J. Adv. Manuf. 95, 4229-4241.Technol. https://doi.org/10.1007/s00170-017-1527-z

Hegab, H, Umer, U., Soliman, M., Kishawy, H.A., 2018. Effects of nano-cutting fluids on tool performance and chip morphology during machining Inconel 718. Int. J. Adv. Manuf. Technol.

96, 3449–3458. https://doi.org/10.1007/s00170-018-1825-0

Jeswiet, J., Kara, S., 2008. Carbon emissions and CES™ in manufacturing. CIRP Ann. - Manuf. Technol. 57, 17–20. https://doi.org/10.1016/j.cirp.2008.03.117

Kaliszer, H., 2003. Grinding technology. Theory and applications of machining with abrasives. Int. J. Mach. Tools Manuf. https://doi.org/10.1016/0890-6955(91)90088-k

Kalpakjian, Serope, and S.S., 1995. Manufacturing engineering and technology, 6th eddition. Addision-Wesley Publishing Company Inc (1992).

Khan, A.M., Jamil, M., Salonitis, K., Sarfraz, S., Zhao, W., He, N., Mia, M., Zhao, G.L., 2019a. Multi-objective optimization of energy consumption and surface quality in nanofluid SQCl assisted face milling. 12, 170-177 Energies. https://doi.org/10.3390/en12040710

Khan, A.M., Jamil, M., Ul Haq, A., Hussain, S., Meng, L., He, N., 2019b. Sustainable machining. Modeling and optimization of temperature and surface roughness in the milling of AISI D2 steel. 2, 267-277. Ind. Lubr. Tribol. https://doi.org/10.1108/ILT-11-2017-0322

Khan, M.M.A., Mithu, M.A.H., Dhar, N.R., 2009. Effects of minimum quantity lubrication on turning AISI 9310 alloy steel using vegetable oil-based cutting fluid. J. Mater. Process. 209, 5573-5583.Technol. https://doi.org/10.1016/j.jmatprotec.2009.05.014

Klocke, F., Eisenblaetter, G., 1997. Dry cutting. CIRP Ann. - Manuf. Technol. https://doi.org/10.1016/S0007-8506(07)60877-4

Lawal, S.A., Choudhury, I.A., Nukman, Y., 2013. A critical assessment of lubrication techniques in machining processes: A case for minimum quantity lubrication using vegetable oil-based lubricant. J. Clean. Prod. 41, 210–221. https://doi.org/10.1016/j.jclepro.2012.10.016

Lee, C.G., Hwang, Y.J., Choi, Y.M., Lee, J.K., Choi, C., Oh, J.M., 2009. A study on the tribological characteristics of graphite nano lubricants. 10, 85-90. Int. J. Precis. Eng. Manuf. https://doi.org/10.1007/s12541-009-0013-4

Lee, K., Hwang, Y., Cheong, S., Choi, Y., Kwon, L., Lee, J., Kim, S.H., 2009. Understanding the role of nanoparticles in nano-oil lubrication. 35, 127-131. Tribol. Lett. https://doi.org/10.1007/s11249-009-9441-7

Li, C., Xiao, Q., Tang, Y., Li, L., 2016. A method integrating Taguchi, RSM and MOPSO to CNC machining parameters optimization for energy saving. 135, 263-275. J. Clean. Prod. https://doi.org/10.1016/j.jclepro.2016.06.097

Li, L., Li, C., Tang, Y., Yi, Q., 2017. Influence factors and operational strategies for energy efficiency improvement of CNC machining. J. Clean. Prod. 161, 220–238. https://doi.org/10.1016/j.jclepro.2017.05.084

Li, L., Yan, J., Xing, Z., 2013. Energy requirements evaluation of milling machines based on thermal equilibrium and empirical modelling. 52, 113-121. J. Clean. Prod. https://doi.org/10.1016/j.jclepro.2013.02.039

Liang, X., Liu, Z., Liu, W., Li, X., 2019. Sustainability assessment of dry turning Ti-6Al-4V employing uncoated cemented carbide tools as clean manufacturing process. J. Clean. Prod. 214, 279–289. https://doi.org/10.1016/j.jclepro.2018.12.196

Lugscheider, E., Knotek, O., Barimani, C., Leyendecker, T., Lemmer, O., Wenke, R., 1999. PVD hard coated reamers in lubricant-free cutting. Surf. Coatings Technol. https://doi.org/10.1016/S0257-8972(98)00775-0

Maruda, R.W., Krolczyk, G.M., Feldshtein, E., Pusavec, F., Szydlowski, M., Legutko, S., Sobczak-Kupiec, A., 2016. A study on droplets sizes, their distribution and heat exchange for minimum quantity cooling lubrication (MQCL). 100, 81-92. Int. J. Mach. Tools Manuf. https://doi.org/10.1016/j.ijmachtools.2015.10.008

Mativenga, P.T., Rajemi, M.F., 2011. Calculation of optimum cutting parameters based on minimum energy footprint. CIRP Ann. - Manuf. Technol. 60, 149–152. https://doi.org/10.1016/j.cirp.2011.03.088

Mehrali, Mohammad, Sadeghinezhad, E., Akhiani, A.R., Tahan Latibari, S., Talebian, S., Dolatshahi-Pirouz, A., Metselaar, H.S.C., Mehrali, Mehdi, 2016. An ecofriendly graphene-based nanofluid for heat transfer applications. 137,555-566. J. Clean. Prod. https://doi.org/10.1016/j.jclepro.2016.07.136

Mia, M., Gupta, M.K., Lozano, J.A., Carou, D., Pimenov, D.Y., Królczyk, G., Khan, A.M., Dhar, N.R., 2019. Multi-objective optimization and life cycle assessment of eco-friendly cryogenic N2 assisted turning of Ti-6Al-4V. J. Clean. Prod. https://doi.org/10.1016/j.jclepro.2018.10.334

Priarone, P.C., Robiglio, M., Settineri, L., 2018. On the concurrent optimization of environmental and economic targets for machining. 190, 630–644. J. Clean. Prod. https://doi.org/10.1016/j.jclepro.2018.04.163

Said, Z., Gupta, M., Hegab, H., Arora, N., Khan, A.M., Jamil, M., Bellos, E., 2019. A comprehensive review on minimum quantity lubrication (MQL) in machining processes using nano-cutting fluids. Int. J. Adv. Manuf. Technol. 105, 2057–2086. https://doi.org/10.1007/s00170-019-04382-x

Sarikaya, M., Güllü, A., 2015. Multi-response optimization of minimum quantity lubrication parameters using Taguchi-based grey relational analysis in turning of difficult-to-cut alloy Haynes 25. J. Clean. Prod. 91, 347–357. https://doi.org/10.1016/j.jclepro.2014.12.020

Sarikaya, M., Güllü, A., 2014. Taguchi design and response surface methodology based analysis of machining parameters in CNC turning under MQL. J. Clean. Prod. 65, 604–616. https://doi.org/10.1016/j.jclepro.2013.08.040

Sarıkaya, M., Yılmaz, V., Güllü, A., 2016. Analysis of cutting parameters and cooling/lubrication methods for sustainable machining in turning of Haynes 25 superalloy. J. Clean. Prod. 133, 172–181. https://doi.org/10.1016/j.jclepro.2016.05.122

Sen, B., Mia, M., Krolczyk, G.M., Mandal, U.K., Mondal, S.P., 2019. Eco-Friendly Cutting Fluids in Minimum Quantity Lubrication Assisted Machining: A Review on the Perception of Sustainable Manufacturing. Int. J. Precis. Eng. Manuf. Technol. https://doi.org/10.1007/s40684-019-00158-6

Sharma, K.A., Tiwari, A.K., Dixit, A.R., 2015. Improved Machining Performance with Nanoparticle Enriched Cutting Fluids under Minimum Quantity Lubrication (MQL) Technique: A Review. Mater. Today Proc. 2, 3545–3551. https://doi.org/10.1016/j.matpr.2015.07.066

Shukla, R.K., Dhir, V.K., 2008. Effect of Brownian Motion on Thermal Conductivity of Nanofluids. 130, p.042406. J. Heat Transfer. https://doi.org/10.1115/1.2818768

Sidik, N.A.C., Mohammed, H.A., Alawi, O.A., Samion, S., 2014. A review on preparation methods and challenges of nanofluids. Int. Commun. Heat Mass Transf. https://doi.org/10.1016/j.icheatmasstransfer.2014.03.002

Su, Y., Gong, L., Li, B., Liu, Z., Chen, D., 2016. Performance evaluation of nanofluid MQL with vegetable-based oil and ester oil as base fluids in turning. Int. J. Adv. Manuf. 83, 2083-2089. Technol. https://doi.org/10.1007/s00170-015-7730-x

U.S., 2009. Carbon, Dioxide Emissions from Energy Sources 2008 Flash Estimate Energy Information Administration Energy-Related Carbon Dioxide Emissions, Mon Energy Rev.

Yıldırım, Ç.V., Sarıkaya, M., Kıvak, T., Şirin, Ş., 2019. The effect of addition of hBN nanoparticles to nanofluid-MQL on tool wear patterns, tool life, roughness and temperature in turning of Ni-based Inconel 625. Tribol. Int. 134, 443–456. https://doi.org/10.1016/j.triboint.2019.02.027

Zhang, F., Duan, C., Wang, M., Sun, W., 2018. White and dark layer formation mechanism in hard cutting of AISI52100 steel. J. Manuf. Process. 32, 878–887. https://doi.org/10.1016/j.jmapro.2018.04.011

Appendix A.1 Components of machining cost rate (h_e) and various components of cost modelling.

Components of machining cost rate (h_e)					
No.	Type of cost	unit	MQL	NFMQL	HNFMQL
1	Labor cost; C_{labor}	¥/hr		15.5	
2	Lighting and HVAC loads are 0.3 and 8.0 kW; C_{HVAC}	¥/hr		6.009	
3	Machine depreciation cost; C_{dep} Machine tool life 12 years;	¥/hr		39.16	
Various components of cost modelling and their values					
1	Energy cost; $\times 10^{-3}$	¥/part	762.3	756.7	745.1
2	Machining cost; $\times 10^{-3}$	¥/part	928.4	927.9	927.6
3	Environmental cost; $\times 10^{-6}$	¥/part	482.0	478.5	471.2
4	Cutting tool cost	¥/part	0.123	0.10	0.082
5	Nanoparticle cost	¥/part	0	0.009	0.023
6	Base-fluid consumption cost	¥/part	0.83	0.83	0.83
	Total cost per part	¥/part	**1.263**	**1.11**	**1.10**
	Total cost per shift	¥/shift	**5709.77**	**5632.39**	**5610.83**

Appendix A.2: Specific values of all metrics used for the overall assessment.

No.	Metrics	MQL	NFMQL	HNFMQL
1	Power (W)	1	0.97407	0.91755
2	Total Energy (J)	1	0.99261	0.97739
3	SEC (J/mm^3)	1	0.99046	0.97075
4	SCE (J/mm^3)	1	0.97261	0.91633
5	SR (μm)	1	0.86154	0.6
6	Temperature (^{o}C)	1	0.88333	0.83333
7	Tool life (mm)	0.6087	0.81159	1
8	Productivity (mm^3)	1	1	1
9	Coolant recyle, disposal	1	1	1
10	Part cleaning	1	1	1
11	Total cost (¥)	1	0.888	0.88
12	Cost per shift (¥)	1	0.98668	0.98279
13	Operator health	0.5	0.5	0.5
14	Carbon emisison (kg)	1	0.99253	0.97759
15	Enviormental cost (¥)	1	0.9917	0.97718

Energy-Based Cost Integrated Modelling and Sustainability Assessment of Al-GnP Hybrid Nanofluid Assisted Turning of AISI52100 Steel

Aqib Mashood Khan[1,2], Munish Kumar Gupta[3], Hussein Hegab[4], Muhammad Jamil[1,2], Mozammel Mia[5], Ning He[1,2*], Qinghua Song[3,6*], Zhanqiang Liu[3,6], Catalin Iulian Pruncu[5,7]

[1]College of Mechanical and Electrical Engineering, Nanjing University of Aeronautics and Astronautics NUAA, Nanjing 21000, China. dr.aqib@nuaa.edu.cn; engr.jamil@nuaa.edu.cn

[2]National Engineering Research Center for Processing of Difficult-to-Machine Materials, College of Electrical and Mechanical Engineering, Nanjing University of Aeronautics and Astronautics NUAA, Nanjing 21000, China.

[3]Key Laboratory of High Efficiency and Clean Mechanical Manufacture, Ministry of Education, School of Mechanical Engineering, Shandong University, Jinan, P.R. China. munishguptanit@gmail.com; https://orcid.org/0000-0002-0777-1559

[4]Mechanical Design and Production Engineering Department, Cairo University, Giza 12163, Egypt; hussien.hegab@uoit.ca

[5]Mechanical Engineering, Imperial College London, Exhibition Road, South Kensington, SW7 2AZ, London, United Kingdom; m.mia19@imperial.ac.uk, https://orcid.org/0000-0002-8351-1871 (M.M.)

[6]National Demonstration Center for Experimental Mechanical Engineering Education, Shandong University, Jinan, P.R. China, ssinghua@sdu.edu.cn, melius@sdu.edu.cn.

[7]Mechanical Engineering, School of Engineering, University of Birmingham, Birmingham B15 2TT, UK, c.pruncu@imperial.ac.uk

Author Contribution Statement

Sr. No.	Contribution	Name of Author
1	Conceptualization;	Aqib Mashood Khan, Munish Kumar Gupta, Mozammel Mia
2	Data curation;	Aqib Mashood Khan, Catalin Iulian Pruncu
3	Formal analysis;	Hussein Hegab, Muhammad Jamil
4	Funding acquisition;	Ning He, Qinghua Song, Zhanqiang Liu
5	Investigation;	Aqib Mashood Khan, Muhammad Jamil
6	Methodology;	Munish Kumar Gupta, Muhammad Jamil, Mozammel Mia
7	Project administration;	Ning He, Qinghua Song, Zhanqiang Liu
8	Resources;	Aqib Mashood Khan, Munish Kumar Gupta
9	Software;	Mozammel Mia, Hussein Hegab, Catalin Iulian Pruncu
10	Supervision;	Ning He, Qinghua Song, Zhanqiang Liu
11	Validation;	Munish Kumar Gupta, Muhammad Jamil
12	Visualization;	Mozammel Mia, Munish Kumar Gupta
13	Roles/Writing - original draft;	Mozammel Mia, Hussein Hegab
14	Writing - review & editing.	Aqib Mashood Khan, Munish Kumar Gupta, Mozammel Mia

Declaration of interests

☐ The authors declare that they have no known competing financial interests or personal relationships that could have appeared to influence the work reported in this paper.

☒The authors declare the following financial interests/personal relationships which may be considered as potential competing interests:

The authors declare that there is no conflict of interest.

Highlights

- Turing of hardened steel under different cooling conditions.
- Implementation of novel energy based cost integrated model.
- Sustainability assessment of cooling conditions.
- Productivity, cost, tool wear and surface roughness were measured.